RESEARCH ON THE HAZARDS ASSOCIATED WITH THE PRODUCTION AND HANDLING OF LIQUID HYDROGEN

By M. G. Zabetakis and D. S. Burgess

* * * * * * * * * * * * report of investigations 5707

UNITED STATES DEPARTMENT OF THE INTERIOR
Fred A. Seaton, Secretary

BUREAU OF MINES
Marling J. Ankeny, Director

DISCLAIMER

This publication has been cataloged as follows:

Zabetakis, Michael G

Research on the hazards associated with the production and handling of liquid hydrogen, by M. G. Zabetakis and D. S. Burgess. [Washington] U. S. Dept. of the Interior, Bureau of Mines [1961]

v, 50 p. illus., tables. 27 cm. (U. S. Bureau of Mines. Report of investigations, 5707)

Bibliographical footnotes.

1. Hydrogen. I. Burgess, D S joint author. II. Title: Hazards associated with handling liquid hydrogen. (Series)

[TN23.U7 no. 5707] 622.06173

U. S. Dept. of the Int. Library

CONTENTS

	Page
Introduction and summary	1
Acknowledgments	2
Definitions and theory	2
Heat transfer to boiling liquids	2
Burning rate theory	7
Transitional (gas phase)	7
Steady-state burning supported by pools of liquid	9
Radiation from hydrogen flames	11
Experimental results and discussion	12
Liquefaction of hydrogen	12
Vaporization of hydrogen	13
Mixing of hydrogen with air	16
Ignition and combustion of hydrogen-air mixtures	18
Burning above liquid pools	27
Burning rate as a function of time	27
Steady burning rate as a function of pool dimension	29
Steady burning rate as determined by fuel properties	31
Phenomenological aspects of pool-supported flames	32
Effect of wind on burning rate	33
Radiation from liquid-supported flames	36
Conclusions and recommendations	37
Appendix I	42
Appendix II	47
Appendix III	49
Appendix IV	50

ILLUSTRATIONS

Fig.		
1.	Heat transfer rates to boiling water at 212° F. for temperature drops between 1 and 1,000° F.	4
2.	Experimental and theoretical heat transfer rates to boiling hydrogen at minus 423° F. for temperature drops between 1° and 1,000° F.	5

ILLUSTRATIONS (Con.)

Fig.		Page
3.	Theoretical heat transfer rates to boiling hydrogen following spillage onto (A) an average soil, (B) moist sandy soil (8 percent moisture), and (C) dry sandy soil	5
4.	Theoretical liquid regression rates following spillage of liquid hydrogen onto (A) an average soil, (B) moist sandy soil (8 percent moisture), and (C) dry sandy soil	8
5.	Theoretical decrease in liquid hydrogen level following spillage onto (A) dry sandy soil, (B) moist sandy soil (8 percent moisture), and (C) an average soil	8
6.	Burning velocity of hydrogen in air at atmospheric pressure and laboratory temperatures	10
7.	Minimum ignition energies for hydrogen-air mixtures at atmospheric pressure	10
8.	Rates of diffusive burning of two liquid hydrocarbon blends	11
9.	Equilibrium concentration of para-hydrogen gas over the temperature range 20-273° K	13
10.	Rate of vaporization of liquid hydrogen from paraffin in a 2.8-inch dewar: Initial liquid depth--6.7 inches	15
11.	Rate of vaporization of liquid nitrogen from paraffin in 6- and 2.8-inch dewars	15
12.	Decrease in liquid hydrogen level following spillage in diked sandy area	16
13.	Height of the visible clouds formed after the rapid spillage of (A) 6.9 and (B) 6.8 liters of liquid hydrogen at 43° and 36° F., respectively, on (A) smooth macadam and (B) gravel	17
14.	Positions of flames above (A) a gravel and (B) a steel plate spill area	18
15.	Hydrogen concentration 2, 4 and 6 seconds following the rapid spillage of 3 liters of liquid hydrogen on a dry macadam surface in a quiescent air atmosphere at 59° F	19
16.	Extent of the flammable mixtures and height of the visible cloud formed after the rapid spillage of 3 liters of liquid hydrogen on a dry macadam surface in a quiescent air atmosphere at 59° F	19
17.	Motion picture sequence (16 frames per second) of the visible cloud and flames resulting from the rapid spillage of 7.8 liters of liquid hydrogen on a gravel surface at 65° F. Ignition source location: 20 inches above gravel	20

ILLUSTRATIONS (Con.)

Fig.		Page
18.	Height and width of visible cloud and flame produced by the rapid spillage of 7.8 liters of liquid hydrogen on a gravel surface at 65° F., 20 inches below an open flame.....	21
19.	Maximum vertical cross-sections of flames produced at various time intervals following spillage of 89 liters of liquid hydrogen on a gravel surface. (Horizontal scale = Vertical scale).....	22
20.	Maximum vertical cross-sections of flames produced by the spillage of 8 to 89 liters of liquid hydrogen. (Horizontal scale = Vertical scale).....	22
21.	Maximum flame height and width produced by the ignition of the vapor-air mixtures formed by the sudden spillage of 2.8 to 89 liters of liquid hydrogen (V_l).....	23
22.	Flame volumes produced by the ignition of the hydrogen vapor-air mixtures formed above pools of liquid hydrogen when ignited between 1.3 and 15.8 seconds after the spillage of the liquid onto a 1/2-inch steel plate or on 4 to 6 inches of loose gravel.....	23
23.	Radiant energy received 47.5 feet from the ignition source following the spillage of (A) 5.0, (B) 8.0 and (C) 7.4 liters of liquid hydrogen; ignition occurred approximately (A) 1.5, (B) 0.75, and (C) 0 seconds following spillage of liquid.....	25
24.	Radiant energy received 110 feet from the ignition source following the spillage of (A) 90, (B) 90, and (C) 89 liters of liquid hydrogen; ignition occurred 4.4, 6.3, and 1.4 seconds, respectively, following spillage of the liquid.....	25
25.	Air and ground temperatures produced by the rapid spillage and ignition of 5.4 liters of liquid hydrogen on a dry macadam surface in a quiescent atmosphere at 62° F. (temperature measurements with bare No. 28 copper-constantan thermocouples).	26
26.	Overpressure (ΔP) produced at a distance of 160 feet by the ignition of the hydrogen-air mixtures formed above pools of liquid hydrogen (54 to 90 liters as noted) when ignited at various times (τ) following spillage of the liquid onto a 1/2-inch steel plate or on 6 inches of loose gravel.....	26
27.	Variation in maximum overpressure with distance produced by the ignition of the hydrogen vapor-air mixtures formed above pools of 15.9 to 90 liters of liquid hydrogen when ignited between 4.4 and 12.5 seconds after spillage of the liquid.....	27

ILLUSTRATIONS (Con.)

Fig.		Page
28.	Burning rates of five liquid fuels in 3-inch pyrex vessel (3.5-inch for UDMH). Vapor pressure 40 millimeters Hg at initial liquid temperature.....	28
29.	Absorption of flame radiations by fuel vapors.....	28
30.	Burning rates of liquid hydrogen and of liquid methane at their boiling points in 6-inch pyrex dewars.....	29
31.	Burning rates of liquid fuels as correlated by Hottel's equation, assuming radiative heat transfer from flame to liquid surface.....	30
32.	Relationship of liquid burning rates at large tray diameter to two physical properties of fuel.....	31
33.	Experimental temperatures in liquid phase compared with theoretical curves for heat input at the liquid surface. Combustion in 30-inch-diameter tray.....	32
34.	Creeping benzene flame on lipless dish (below) compared with noncreeping flame on dish with 1/2-inch lip.....	34
35.	Side views and under views of benzene flames in 6-inch-diameter dish. (a) Flame undisturbed; (b) Radial draft induced by chimney; (c) Flame torn from rim of tray.....	35
36.	Burning of liquid hydrogen in dewars of three diameters (reconstructed from flame radiation data)...	36
37.	Variation in distance to unbarricaded inhabited buildings (Class 950 materials) and r_2 cal./cm.^{2} with mass (M) of liquid hydrogen.....	39
38.	Variation in above ground unbarricaded intermagazine separation (Class 950 materials) and M with mass (M) of liquid hydrogen.....	41
39.	Schematic layout of Collins Cryostat and related equipment.....	48
40.	Compensated thermocouple for radiation measurements.	50

TABLES

1.	Properties of hydrogen.....	42
2.	Comparison of measured flame temperatures with values calculated from percentages of heat radiated.....	42
3.	Absorption of flame radiations by 0.116-inch pathlength of liquid fuel in cell with CaF_2 windows...	43
4.	Influence of cross wind on fuel consumption rates in trays (fuel level about 1/8-inch below rim of tray).....	43

TABLES (Con.)

Page

5. Preliminary measurements of radiative heat transfer in methanol flames..... 44
6. Radiation by gaseous diffusion flames..... 44
7. Emissivity of hydrogen diffusion flame on 16-inch burner..... 45
8. Radiation of liquid-supported diffusion flames..... 45
9. Percentage absorption of flame radiations by water vapor (steam at 100° C.) in cells with CaF_2 windows 46
10. Proposed quantity-distance tables for liquid hydrogen 46

RESEARCH ON THE HAZARDS ASSOCIATED WITH THE PRODUCTION AND HANDLING OF LIQUID HYDROGEN[1/]

by

M. G. Zabetakis[2/] and D. S. Burgess[2/]

INTRODUCTION AND SUMMARY

The use of liquid hydrogen as a high-energy fuel introduces numerous hazards not ordinarily associated with the use of other more conventional fuels. These hazards are attributable to the unique properties of hydrogen in the liquid and gas states (table 1). Since little work has been conducted on explosion and related hazards of cryogenic fuels, a research program was undertaken to obtain basic data on such dangers for hydrogen and other combustibles under these conditions. These data were used to outline emergency procedures for protecting personnel and equipment when an accidental spillage of liquid hydrogen occurs and to establish a quantity-distance table for the storage of this fuel.

The vaporization of liquid hydrogen from a surface is treated as a problem in heat transfer theory. Two extreme cases are briefly considered: (1) The transfer of heat occurs at constant temperature drop between the boiling liquid and the hot surface, and (2) the transfer of heat is limited by the rate at which it can flow to the surface from a hot insulating medium. The available data indicate that the former case (1) is applicable when vaporizing from a conducting surface and, initially, when vaporizing from an insulating medium; the latter case (2) is applicable after initial flash vaporization has occurred from the insulating medium. The vaporization rate determines in part the rate at which flammable hydrogen vapor-air mixtures are formed above a spill area. However, the rates at which heat is transferred to the vapor, and air is brought in contact with it also are of importance. Accordingly, the distribution of flammable mixtures above a spill area was determined experimentally. In general, flammable mixtures were found to be both above and within the visible vapor cloud.

1/ Work on manuscript completed January 1960. The work upon which this report is based was done by the Bureau of Mines, U.S. Department of the Interior, under U.S. Air Force Delivery Order No. (33-616) 58-5 during the period January 1958 to December 1959. A report of this work is also given in WADD Technical Report 60-141.

2/ Supervisory physical chemist, project coordinator, Explosives Research Laboratory, Bureau of Mines, Pittsburgh, Pa.

The hazards associated with the ignition of hydrogen vapor-air mixtures above a liquid hydrogen spill area were determined by (1) igniting the vapors above a dewar and (2) igniting the vapor-air mixtures above a spill area at various times following spillage of varying amounts (up to 90 liters) of liquid hydrogen. Flame height and width measurements were made from motion pictures of the resultant flames. In addition, radiant-energy and overpressure measurements were made at various distances from the flame. While the flame radiation was found to represent an appreciable amount of the available energy, the overpressure produced by the rapid combustion of hydrogen above a spill area was quite small.

Burning-rate measurements were conducted on pools of various liquid fuels including hydrogen. These were used to correlate burning rate with the heat feedback to a pool to maintain steady vaporization and combustion.

Finally, the results of this study were used to compile a table of distances for the storage of liquid hydrogen and to outline emergency procedures for the protection of personnel and equipment when an accidental spillage of hydrogen occurs.

ACKNOWLEDGMENTS

The authors wish to acknowledge the cooperation of Lt. J. C. Henry and L. C. Dickey, U.S. Air Force, who acted as project engineers for the Wright Air Development Division.

DEFINITIONS AND THEORY

Heat Transfer to Boiling Liquids

Heat may be transferred to a liquid which is at temperatures below or equal to its boiling point.[3] At liquid temperatures below the boiling point, vapor bubbles are formed at the hot surface and rise into the liquid. However, the bubbles may collapse as vapor condenses in the cooler portion of the liquid. At liquid temperatures equal to the boiling point, bubbles that are formed at the hot surface do not collapse after leaving it. The phenomena associated with this latter process are of sufficient importance to the present study to warrant a brief review of the current theory of boiling. An excellent comprehensive review of this subject was presented recently by Westwater.[4]

The transfer of heat to a boiling liquid may be accomplished by one of several mechanisms. In the first, with relatively small temperature differences between the heat source and the liquid, heat is transferred principally by natural convection; heat-transfer rates are normally somewhat greater than those predicted by Newton's law of cooling ($q/A = h \Delta T$). In the second, vapor

---

3/ McCabe, Warren L., and Smith, Julian C., Unit Operations of Chemical Engineering: McGraw-Hill Book Co., New York, N.Y., 1956, pp. 482f.

4/ Westwater, J. W., Boiling Heat Transfer: American Scientist, 47, 1959, pp. 427-446.

bubbles are produced at such a rate that the natural convection currents are augmented and the heat-transfer rate increases with the temperature difference between the heat source and the liquid at a much greater rate than that predicted by Newton's law. This is the temperature difference region in which nucleate boiling occurs. The heat-transfer rate continues to increase as the temperature difference between the heat source and the liquid increases until a large part of the source is covered with a blanketing vapor. Since this blanket insulates the heat source, a temperature difference is ultimately reached which yields a maximum heat-transfer rate for this mechanism. The temperature difference at which this occurs is termed the critical temperature drop. A further increase in the temperature drop causes the heat-transfer rate to decrease until a minimum value is attained at the Leidenfrost point. With this temperature difference, the insulating vapor blanket is continuous so that heat passes to the liquid through the vapor only. At still higher values of temperature difference, the heat-transfer rate again increases with the temperature difference. This is the region of film boiling. The transition region between the critical temperature drop and the Leidenfrost point is termed the metastable film boiling region.

Each of the above regions is illustrated in figure 1 which was constructed from the data of Nukiyama[5] [6] who reportedly conducted the first scientific study of boiling[7] with water. Similar data and a theoretical curve are given in figure 2 for liquid hydrogen;[8] the experimental data were obtained with smooth, rough and greased heated horizontal Karma (Ni 73%, Cr 20% + Al + Fe) surfaces.

Thus far, we have considered only the rate at which heat can be transferred to a boiling liquid as a function of the nature of the surface and the constant temperature difference between the liquid and the hot surface. However, in many applications a constant temperature difference cannot be established and a variable (that is, time-dependent) heat-transfer rate is obtained. With insulating materials, for example, the heat-transfer rate may be controlled by the rate at which heat flows to the surface. To investigate such materials, consider a semi-infinite insulating medium at an initial temperature T_i. If the temperature of the free surface is suddenly lowered and kept at T_o, the temperature distribution within the insulating material can be found by solving the linear heat flow equation:[9]

5/ Nukiyama, Shiro, Maximum and Minimum Values of Heat Transmitted From Metal to Boiling Water under Atmospheric Pressure: Jour. Soc. Mech. Eng., Japan, 37, No. 206, 1934, pp. 367-374.

6/ McAdams, W. H., Addoms, J. N., Rinaldo, P. N., and Day, R. S., Heat Transfer From Single Horizontal Wires to Boiling Water: Chem. Eng. Prog., 44, No. 8, 1948, pp. 639-646.

7/ See footnote 4.

8/ Class, C. R., Dehaan, J. R., Piccone, M., and Cost, R. B., Pool Boiling Heat Transfer to a Boiling Liquid: Wright Air Development Center TR 58-528 (ASTIA AD 214 256), 1958.

9/ Carslaw, H. S., and Jaeger, J. C., Conduction of Heat in Solids: Clarendon Press, Oxford, England, 1959.

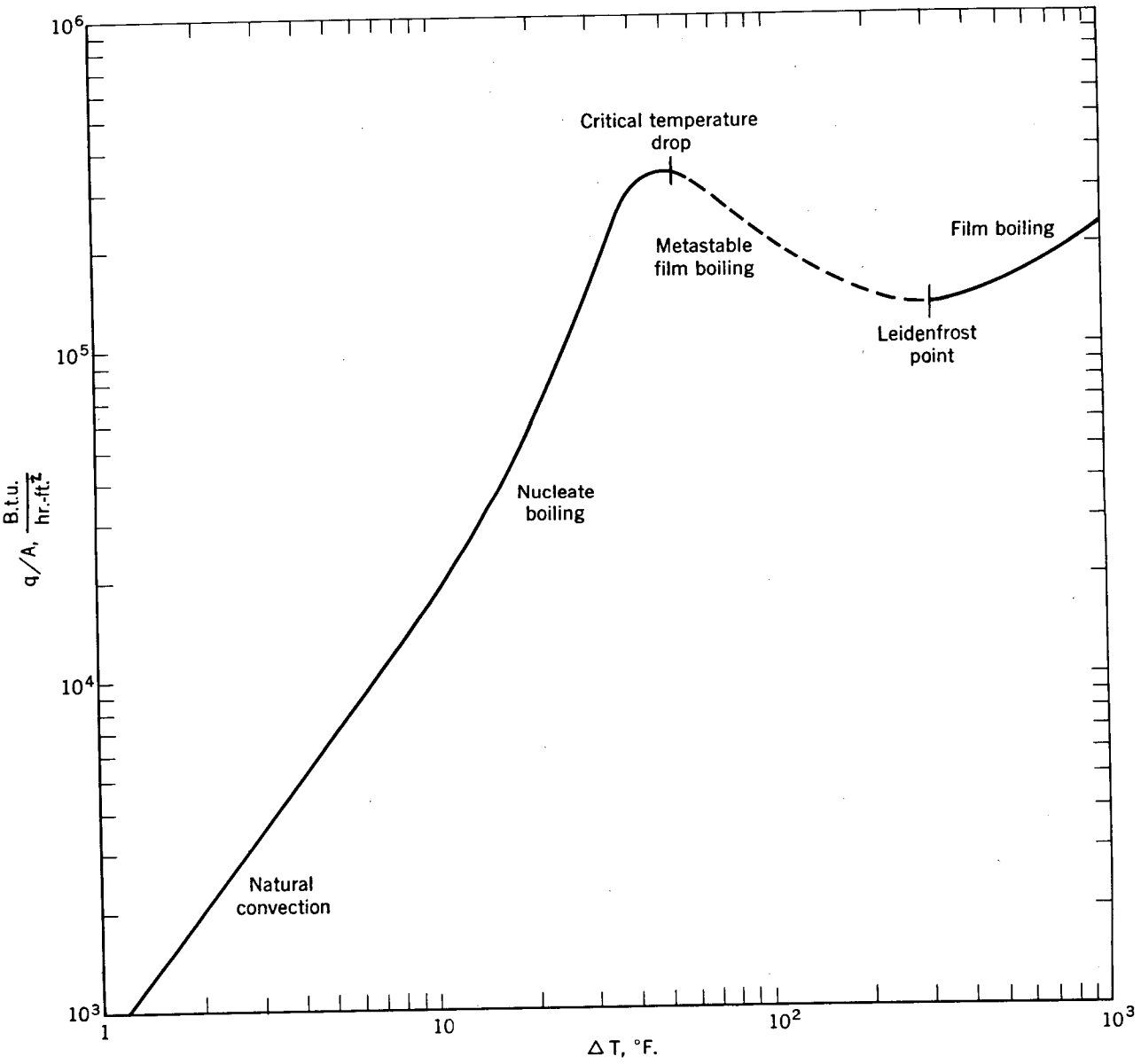

FIGURE 1. - Heat Transfer Rates to Boiling Water at 212° F. for Temperature Drops Between 1 and 1000° F.

$$\frac{\partial^2 T}{\partial y^2} - \frac{1}{k} \cdot \frac{\partial T}{\partial t} = 0 \qquad (1)$$

with $T = T_i$ for $y > o$ and $T = T_o$ for $y = 0$ when $t = 0$.

Under these conditions, the (absolute) temperature in the material is:

$$T = T_o + (T_i - T_o) \operatorname{erf} \frac{y}{2\sqrt{kt}} \qquad (2)$$

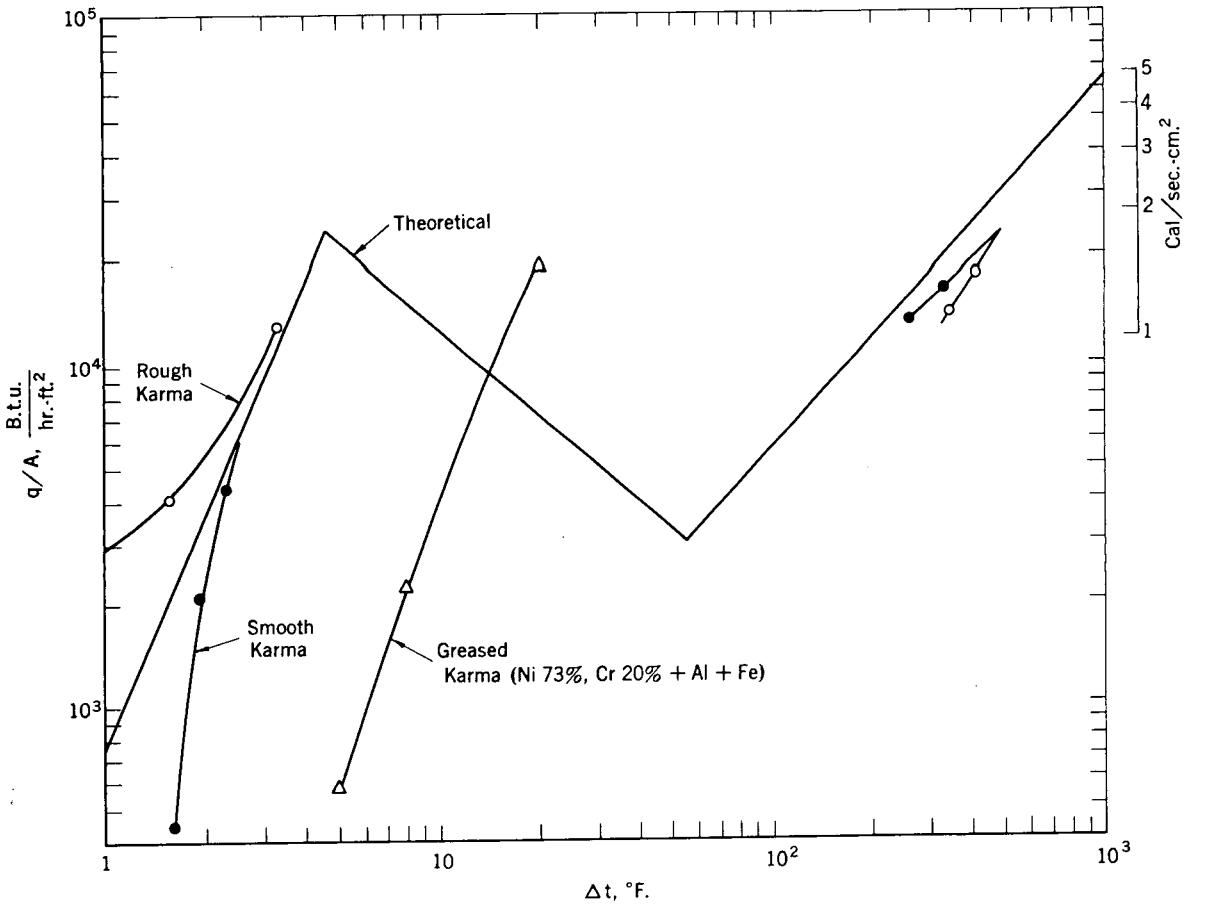

FIGURE 2. - Experimental and Theoretical Heat Transfer Rates to Boiling Hydrogen at -423° F. for Temperature Drops Between 1 and 1000° F.

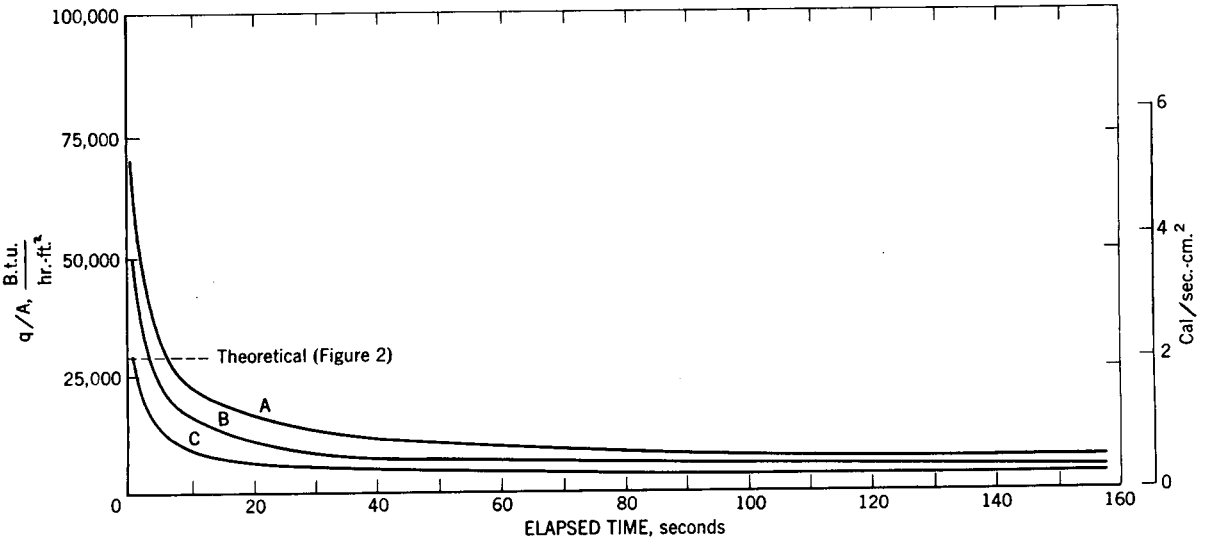

FIGURE 3. - Theoretical Heat Transfer Rates to Boiling Hydrogen Following Spillage Onto (A) an Average Soil, (B) Moist Sandy Soil (8% moisture), and (C) Dry Sandy Soil.

where

$$\operatorname{erf} \frac{y}{2\sqrt{kt}} = \frac{2}{\sqrt{\pi}} \int_{o}^{y/2 \cdot \sqrt{kt}} e^{-z^2} dz$$

$k = \frac{K}{\rho_s c}$ is the thermal diffusivity of the insulating material

K is the thermal conductivity

ρ_s is the density

c is the specific heat

y is the distance below the surface of the semi-infinite solid

and t is the elapsed time from the instant the surface temperature is lowered to T_o.

The heat transfer rate at the surface is

$$\frac{q}{A} = -K \left[\frac{\partial T}{\partial y}\right]_{y = o} \tag{3}$$

Since the temperature gradient is

$$\frac{\partial T}{\partial y} = \frac{T_i - T_o}{(\pi kt)^{1/2}} \exp\left(-\frac{y^2}{4kt}\right) \tag{4}$$

then, at the surface

$$\left|\frac{q}{A}\right| = K \cdot \frac{T_i - T_o}{(\pi kt)^{1/2}}. \tag{5}$$

This equation indicates that the heat-transfer rate varies inversely with the square root of the elapsed time, t. Examples of this behavior are shown in figure 3 in which q/A is plotted as a function of t for liquid hydrogen at 20.4° K. in contact with three soils at an initial temperature of 300° K.

The rate at which a liquid vaporizes (liquid regression rate) when the above heat is absorbed at its boiling point is given by:

$$\dot{y} = \frac{\dot{V}}{A} = \frac{\dot{m}}{\rho A} = \frac{1}{\rho L} \cdot \frac{q}{A}. \tag{6}$$

Using equation (5) this becomes

$$\dot{y} = \frac{K}{\rho L} \cdot \frac{T_i - T_o}{(\pi k t)^{1/2}} \tag{7}$$

where L is the heat of vaporization per unit mass and ρ is the density of the liquid.

Assuming K, ρ, L and k to be independent of T, we get by integration

$$\Delta y = \frac{2K}{\rho L} \cdot \frac{T_i - T_o}{(\pi k)^{1/2}} \; t^{1/2} \tag{8}$$

where Δy is the change in liquid level in elapsed time, t. Figures 4 and 5 give, respectively, the variation in $\dot{y}$ and Δy with t, for liquid hydrogen in contact with the three surfaces considered in figure 3.

A comparison of figures 2 and 3 indicates that the heat-transfer rates given in the latter figure are too large for elapsed times near the origin (from equation (5), q/A increases indefinitely as t approaches zero). Using the theoretical curve for hydrogen in figure 2 to establish an upper value for q/A for elapsed times near the origin (broken curve in figure 3), the curves in figures 3, 4, and 5 can be modified to yield somewhat more realistic values near the origin.

The above analysis assumes the specific surface area is equal to the plane projected area. However, if this is not the case, $\dot{y}$ and Δy should be multiplied by a factor R defined as

$$R = \frac{\text{total surface area}}{\text{projected area}} \geq 1$$

so that

$$\dot{y} = R \cdot \frac{K}{\rho L} \cdot \frac{T_i - T_o}{(\pi k t)^{1/2}} \tag{9}$$

and

$$\Delta y = R \cdot \frac{2K}{\rho L} \cdot \frac{T_i - T_o}{(\pi k)^{1/2}} \; t^{1/2}. \tag{10}$$

Thus, vaporization rates can be increased in a particular spill area merely by increasing the specific surface area (that is, by the use of a pebble bed); conversely, vaporization rates can be decreased by the use of small smooth diked areas.

Burning Rate Theory

Transitional (Gas Phase)

Hydrogen normally burns in air at a rate that is determined by the composition of the resultant hydrogen-air mixture. Typical burning velocity data

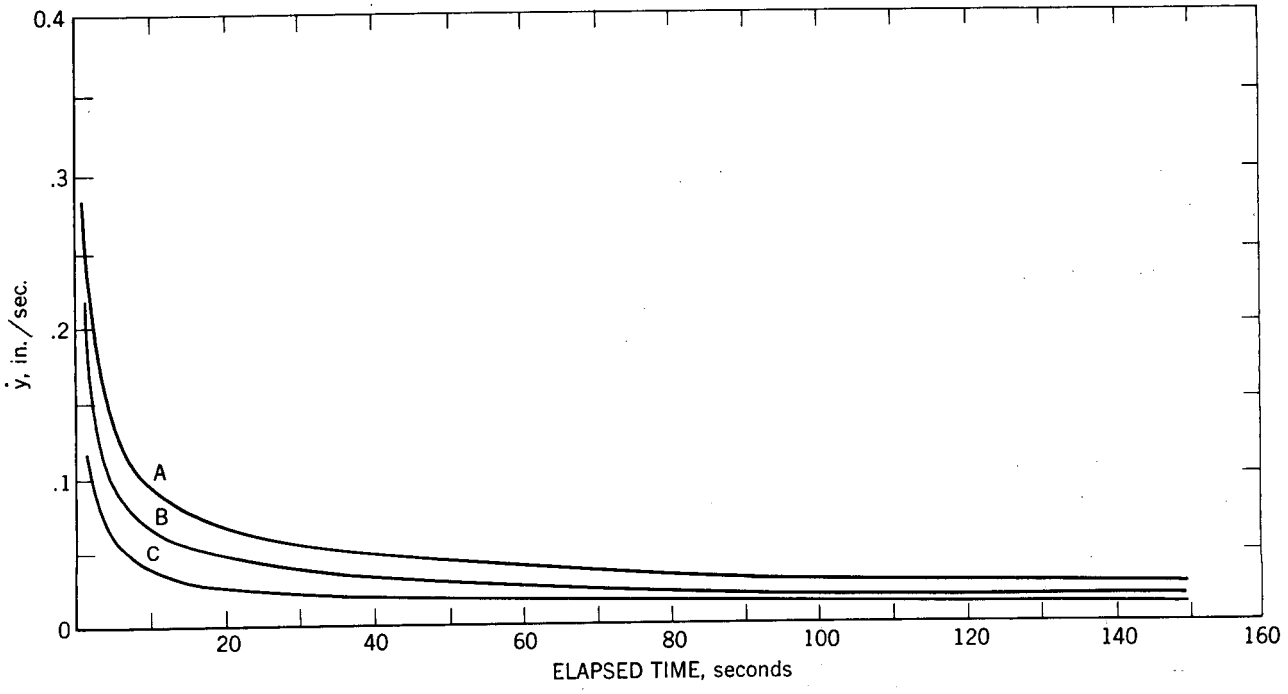

FIGURE 4. - Theoretical Liquid Regression Rates Following Spillage of Liquid Hydrogen Onto (A) an Average Soil, (B) Moist Sandy Soil (8% moisture), and (C) Dry Sandy Soil.

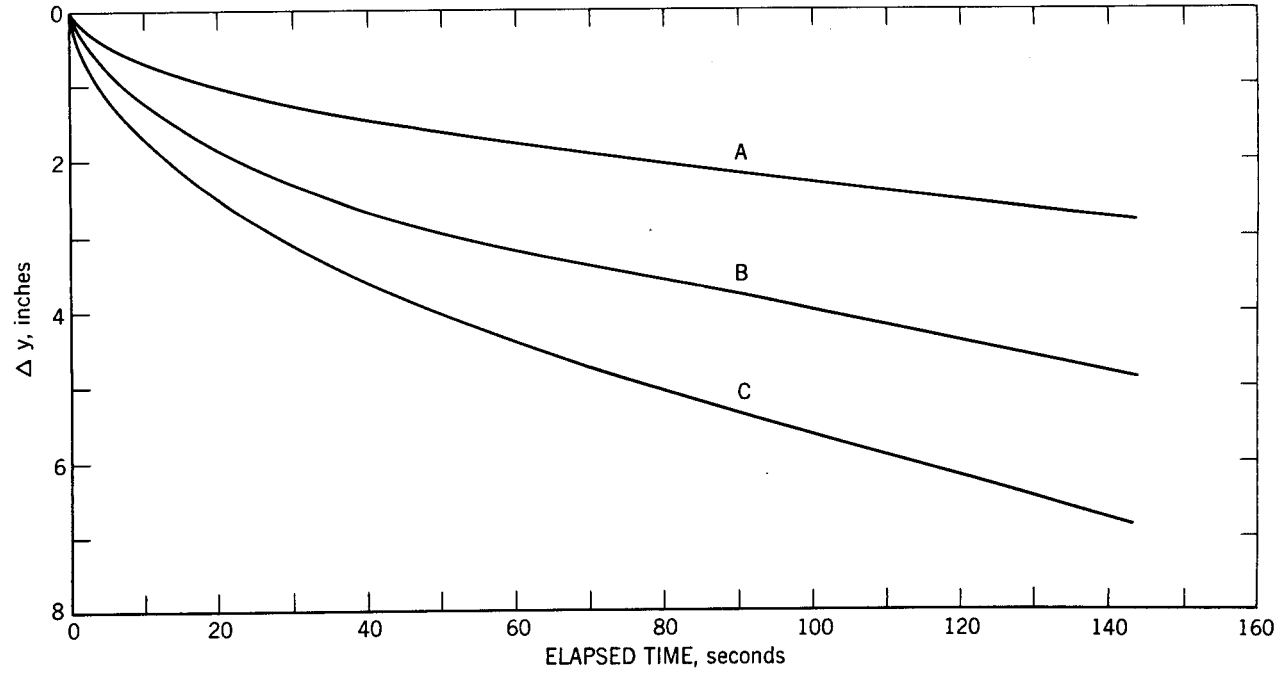

FIGURE 5. - Theoretical Decrease in Liquid Hydrogen Level Following Spillage Onto (A) Dry Sandy Soil, (B) Moist Sandy Soil (8% moisture), and (C) an Average Soil.

for hydrogen at atmospheric pressure and laboratory temperatures are given in figure 6;[10] the burning velocity is the velocity of the flame front relative to the unburned gas. The speed with which a flame moves through space depends on the relative motion of the gas as well as the burning velocity. For this reason, flame speeds considerably in excess of the maximum burning velocity are readily obtained; such speeds may approach the local speed of sound in the burning mixture. The minimum energy requirements for the ignition of hydrogen-air mixtures are given in figure 7.[11] These energy values are in the range 0.02 to 1 millijoule. However, if the source energy is increased sufficiently, a detonation may be initiated. In any case, large amounts of energy can be liberated in a very short time when hydrogen-air mixtures are ignited so that adequate precautions must always be taken to prevent the accumulation of such mixtures in enclosed spaces.

Steady-State Burning Supported by Pools of Liquid

The problem of steady-state burning has been approached by burning fuels in open trays. A useful precedent for this work was encountered in a paper by Blinov and Khudiakov[12] in which the authors showed that aviation gasoline in trays burned at a (linear) rate which was diameter-independent in the diameter range of 3 to 70 feet (figure 8). The chief question to be settled in this part of the program was whether Blinov and Khudiakov's finding could be generalized to include the case of liquid hydrogen. The work was facilitated further by Hottel's analysis of the Russian work.[12] In this work, radiation from the flame to unit area of liquid surface was written

$$\frac{q}{\pi d^2/4} = \sigma F(T_F^4 - T_B^4)(1 - e^{-Kd}). \qquad (11)$$

The shape of the curve of burning rate (fuel-vaporization rate) versus tray diameter is determined primarily by the term $(1 - e^{-Kd})$ in which K is the opacity coefficient and d the diameter.[14] On this basis a limiting value of burning rate is attained when e^{-Kd} becomes effectively zero. For hydrocarbon flames the value of K is found from burning rates at two tray diameters to be of the order of 0.6-0.9 ft.$^{-1}$, so that e^{-Kd} approaches zero when d is of the order of 4 feet.

10/ Lewis, B., and von Elbe, G., Combustion, Flames and Explosions of Gases: Academic Press, Inc., New York, N.Y., 1951, p. 460.

11/ Work cited in footnote 10, p. 414.

12/ Blinov, V. I., and Khudiakov, G. N., Certain Laws Governing the Diffusivity Burning of Liquids: Acad. Nauk, U.S.S.R. Doklady, 113, 1957, 1094-1098.

13/ Hottel, H. C., Review of Certain Laws Governing Diffusive Burning of Liquids: Fire Res. Abs. and Rev., 1, 1958, pp. 41-44.

14/ The factors σ (Stefan-Boltzmann constant), F (shape Factor), T_f (flame temperature), and T_B (liquid surface temperature, assumed to be at the boiling point) should be effectively constant at large diameters.

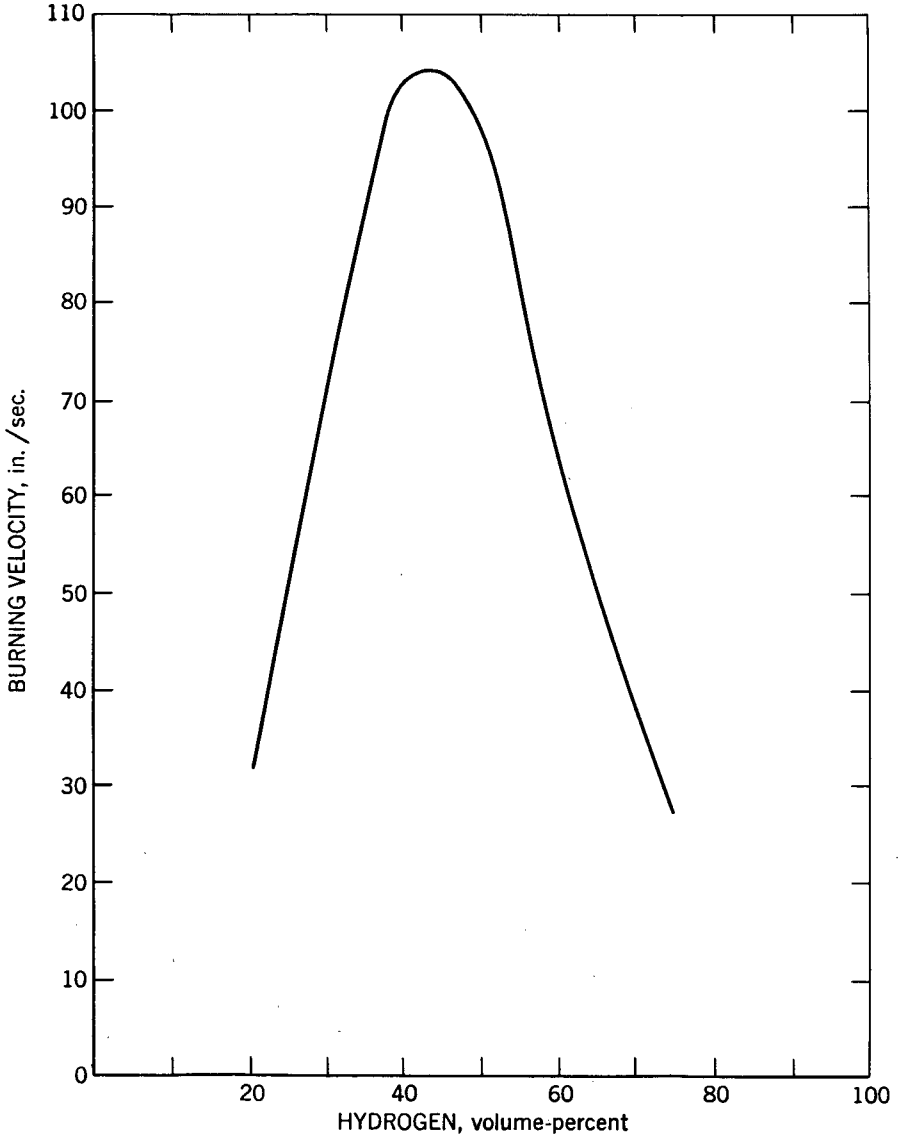

FIGURE 6. - Burning Velocity of Hydrogen in Air at Atmospheric Pressure and Laboratory Temperatures.

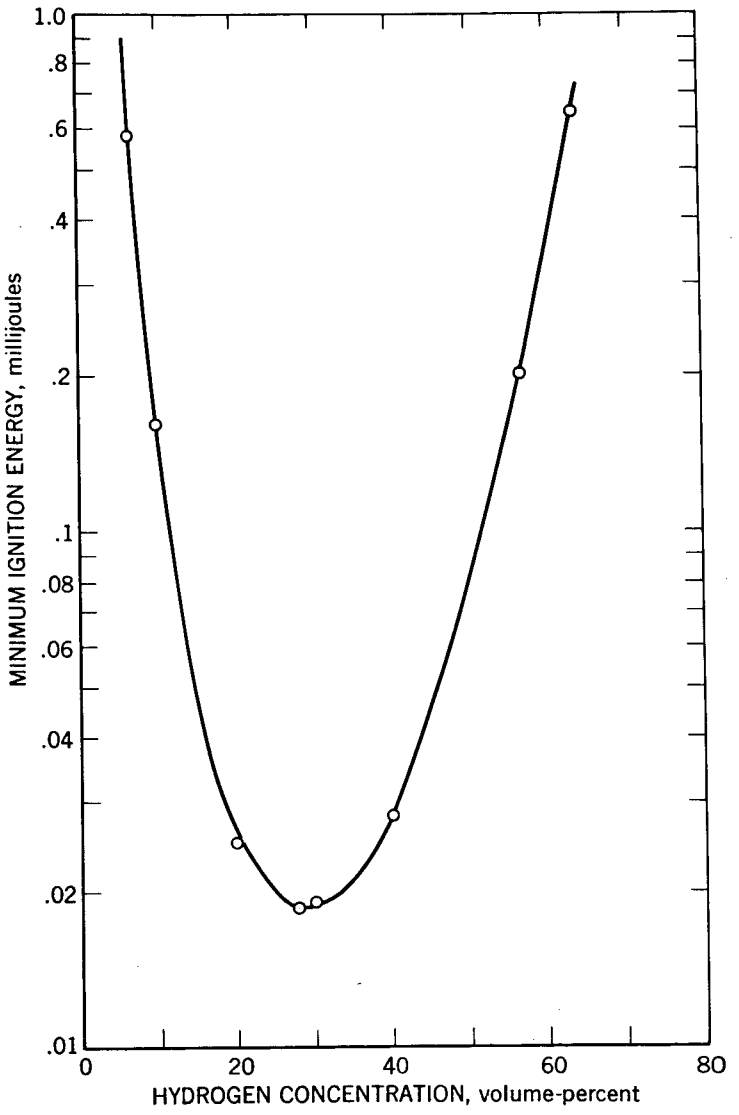

FIGURE 7. - Minimum Ignition Energies for Hydrogen-Air Mixtures at Atmospheric Pressure.

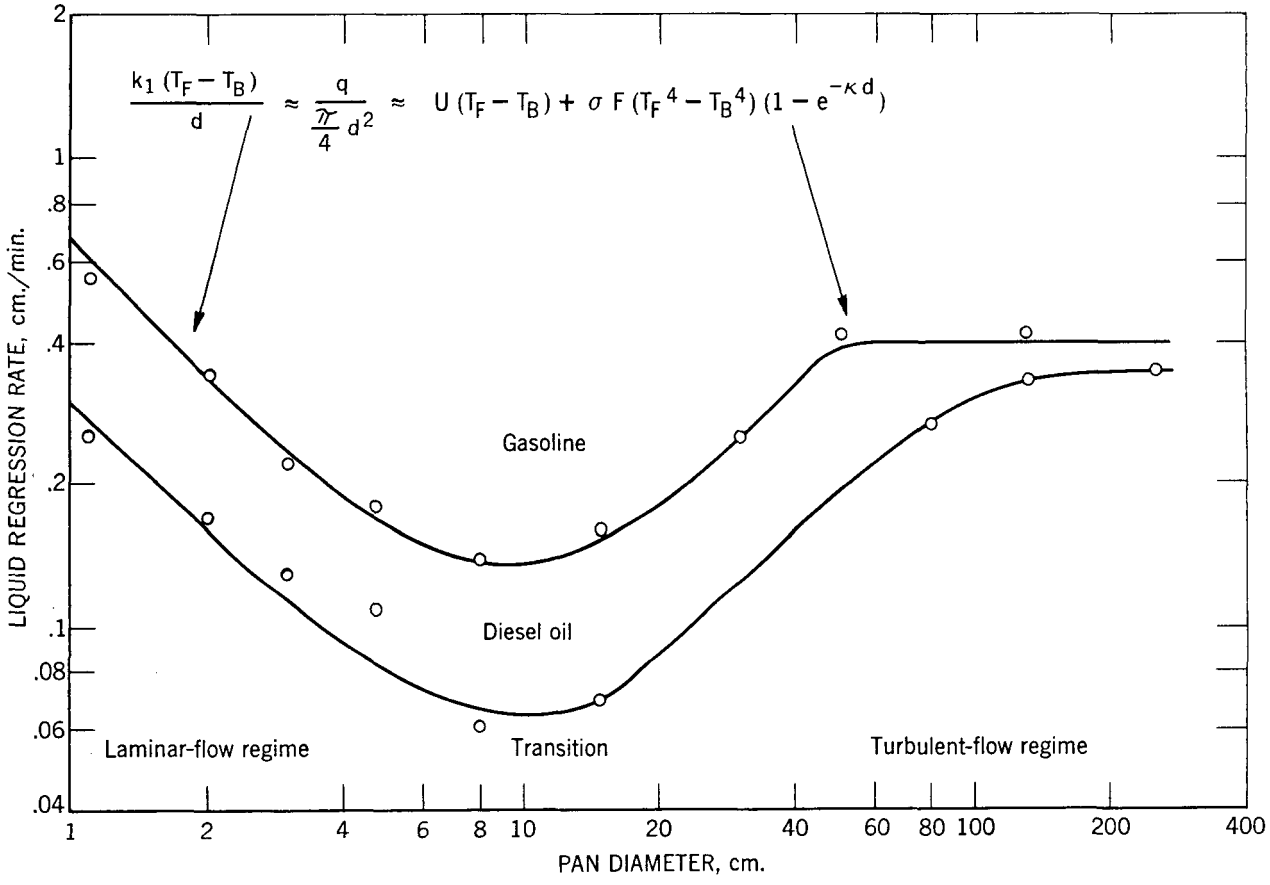

FIGURE 8. - Rates of Diffusive Burning of Two Liquid Hydrocarbon Blends. (Data Extracted From Ref. 1).

Radiation From Hydrogen Flames

In estimating the transfer of heat from a flame to its surroundings, one commonly deals with the same factors as presented in equation (11) for estimation of radiation flux to the liquid surface. It is normally assumed that radiation emanates almost exclusively from the luminous envelope of the fire which is taken to be a grey body and that emission from the hot (nonluminous) burned gases is negligible. The flame size and shape can be taken from photographs and flame temperature and emissivity, or opacity, measured by standard methods.15/ However, in the case of hydrogen flames where there is no emitting surface that even approximates a grey body, the evaluation of these factors would present formidable problems.

It is therefore assumed that each size of flame radiates a characteristic percentage of its total heat of combustion to the surroundings and that this percentage approaches constancy as the size of flame is increased. This is, in fact, a backward step in the description of flames, and, as has been

15/ Rasbash, D. J., Rogowski, Z. E., and Stark, G. W. V., Properties of Fires of Liquids: Fuel, 35, 1956, pp. 94-107.

pointed out, every flame eventually disposes of all of its heat of combustion by radiative processes.16/ However, the percentage of heat radiated from the combustion zone itself is exactly as fundamental a property as the flame temperature, since it is almost exclusively by radiation that the flame's surface temperature is reduced from the theoretical thermochemical value. An interesting illustration of this point is given in table 2, wherein the second column lists measured flame temperatures and the fourth column lists the expected temperatures, based on stoichiometric burning and measured radiation to the surroundings. The small deficiency of the measured values could reflect an incompleteness of combustion at the surface of the luminous zone. The flame temperature, as used in equation (11), can be assumed constant with increasing flame size only if the percentage of heat radiated is constant, which in turn requires that the flame approach constant geometric configuration.

EXPERIMENTAL RESULTS AND DISCUSSION

Liquefaction of Hydrogen

Hydrogen and other gases can be liquefied directly or indirectly by the use of one or both of two methods.17/ The first, or internal, work method employs the Joule-Thomson effect; the second, or external, work method utilizes the reversible expansion of the gas to perform external work. In this investigation, hydrogen was liquefied in a modified Collins liquefier (cryostat)18/ in which helium was cooled in the two expansion engines and was then used to liquefy the hydrogen directly in the cryostat. The unconverted hydrogen (at room temperature, hydrogen consists of a mixture of 25 percent parahydrogen and 75 percent orthohydrogen (figure 9))19/ was withdrawn from the cryostat with an evacuated transfer line (appendix II). Converted hydrogen obtained from an external source was used in conducting the tests in which more than 50 liters of liquid was used.

In addition to the usual hazards associated with the use of gaseous hydrogen, a new hazard exists when preparing and using the liquid, since air in contact with liquid hydrogen will condense and form "ice" crystals. Flash vaporization of the hydrogen may then cause the formation of slurries containing a relatively large amount of such ice. Still another hazard is created if hydrogen is transferred into open dewars which have been precooled to temperatures below the boiling point of oxygen (minus 297° F.), since oxygen may condense in such dewars and form shock-sensitive mixtures upon addition of liquid hydrogen.

16/ Discussion following talk by M. Zabetakis at First International Symposium on Fire Research, Washington, D. C., November 9-10, 1959.

17/ Jackson, L. C., Low Temperature Physics: Methuen and Co., Ltd., London, England, 1955.

18/ Collins, S., Ch. in Encyclopedia of Physics: Springer-Verlag, Germany, 1956, 14, pp. 132-133.

19/ Farkas, A., Orthohydrogen, Parahydrogen and Heavy Hydrogen: The University Press, Cambridge, England, 1935.

Vaporization of Hydrogen

If unconverted liquid hydrogen is stored at its boiling point (minus 423° F.) the orthohydrogen is slowly converted to parahydrogen.[20] The rate of the noncatalytic conversion is given by

$$\frac{dN_o}{dt} = kN_o^2 \qquad (12)$$

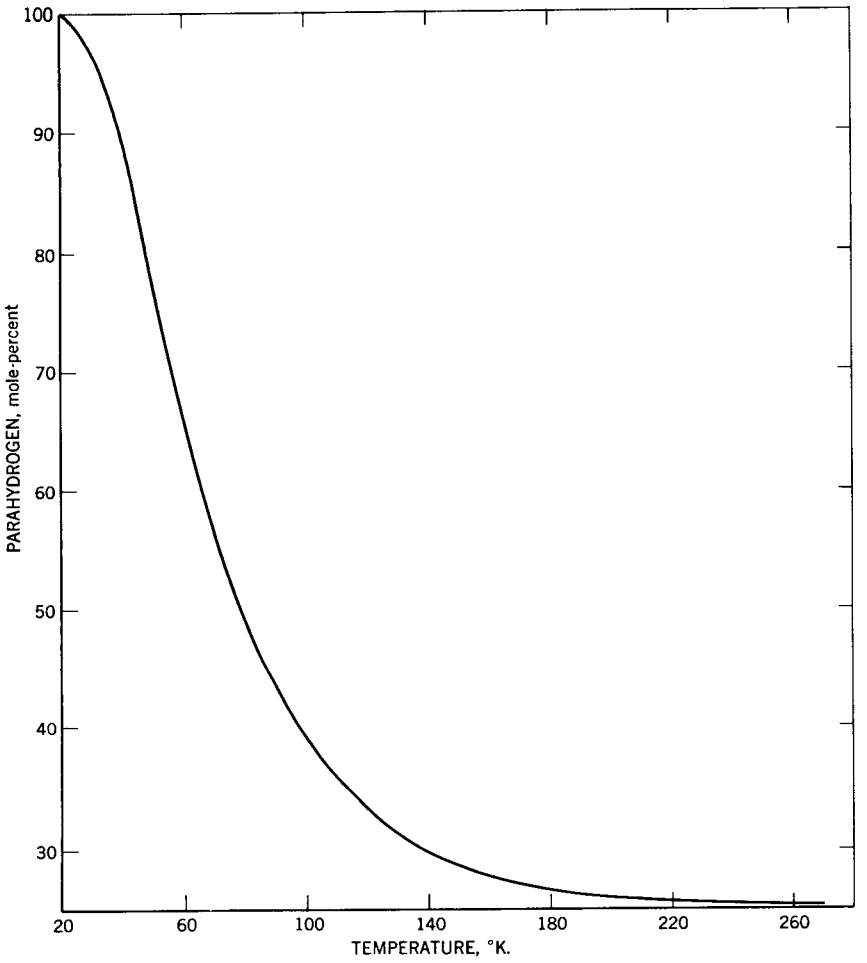

FIGURE 9. - Equilibrium Concentration of Parahydrogen Gas Over the Temperature Range 20-273° K.

where N_o is the mole fraction of orthohydrogen and k is the rate constant (approximately 0.012/hr.). Approximately 339 calories are liberated per mole of hydrogen in the conversion process.[21] [22] This is enough heat to vaporize 1.59 moles of the liquid. To prevent such vaporization losses, normal hydrogen must be converted if it is to be stored for an appreciable period. However, conversion may not be necessary if the liquid is to be used immediately after production.

As with any other liquid, the rate at which hydrogen is vaporized at its boiling point is

$$\frac{dn}{dt} = \frac{1}{L} \cdot \frac{dQ}{dt} \qquad (13)$$

where L is the heat of vaporization (ca. 213 cal./mole[23]) and dQ/dt (that is, q) is the rate

20/ Grilly, E. R., The Liquefaction and Storage of Partially Converted Liquid Hydrogen: Rev. Sci. Instr., 24, No. 1, January 1953, pp. 1-4.

21/ Scott, R. B., Cryogenic Engineering: D. Van Nostrand Co., Inc., New York, N.Y., 1959.

22/ Woolley, H. W., Scott, R. B., and Brickwedde, F. G., Compilation of Thermal Properties of Hydrogen in Its Various Isotopic and Ortho-Para Modifications: Jour. Res. Nat. Bureau Standards, 41, 1948, 379, RP 1932.

23/ See footnote 22.

at which heat is absorbed by the liquid. As noted above under "Definitions and Theory, (Heat Transfer to Boiling Liquids)" the rate at which heat is absorbed from a hot surface depends on the nature of the contacting surface and on the temperature difference between the surface and the boiling liquid. At normal ambient temperatures, the rate of flow of heat into the liquid starts at a high value but decreases as the surface temperature is lowered until the Leidenfrost point is reached. A further decrease in the surface temperature will cause the heat-transfer rate to increase until the critical temperature drop is reached and then to decrease again if the temperature drop falls below the critical value (figure 2). Thus, in theory we can calculate the rate at which liquid hydrogen is vaporized from unit area of a particular surface, if we know the temperature drop between the surface and the liquid. Unfortunately, this temperature drop is not readily available in cases involving accidental spills.

The rate at which liquid hydrogen was vaporized from the surface of a block of paraffin wax cast in a 2.8-inch glass dewar was determined by measuring the rates of gas evolution with a dry-gas meter at various times following spillage of the hydrogen into the dewar. These are expressed as liquid regression rates ($\dot{y}$) in figure 10; they are represented quite adequately by the theoretical curve given by equation (7) for insulating materials. Similar data are given for liquid nitrogen in figure 11. These also show quite conclusively that liquid regression rates of cryogenic fluids can be calculated at times that are greater than those corresponding to the initial flash vaporization rates by assuming the heat flux to the liquid is limited by the rate at which heat can flow to the surface of the insulating material. However, the initial flash vaporization rates are not limited by the conduction of heat through the insulating material and are probably determined by the film- and nucleate-boiling mechanisms discussed previously under "Definitions and Theory." The general trend in the region of violent boiling (before the surface temperature approaches that of the liquid) is given by a broken curve in figure 10; the position of this curve is not especially significant.

The time required to vaporize a pool of liquid hydrogen from the surface of an insulating material is given by equation (8); the decrease in liquid level with elapsed time for liquid hydrogen in contact with three soils is given in figure 5. The curve for moist sandy soil is redrawn in figure 12 which also gives large scale vaporization data reported recently.24/ Since there is considerable spread in the experimental data, we can only conclude that some of the values fall within the range predicted by the theoretical curve.

A crude indication of the variation in the initial vaporization rates from various surfaces is shown in figures 13 and 14 which were constructed from motion pictures of hydrogen spill tests. In the first figure, the heights of the visible clouds that were formed after the rapid spillage of approximately the same quantities of liquid hydrogen on a smooth macadam

24/ Arthur D. Little, Inc., Interim Report on an Investigation of Hazards Associated With Liquid-Hydrogen Storage and Use: Contract No. AF 18(600)-1687, C-61092, Jan. 15, 1959, pp. 92.

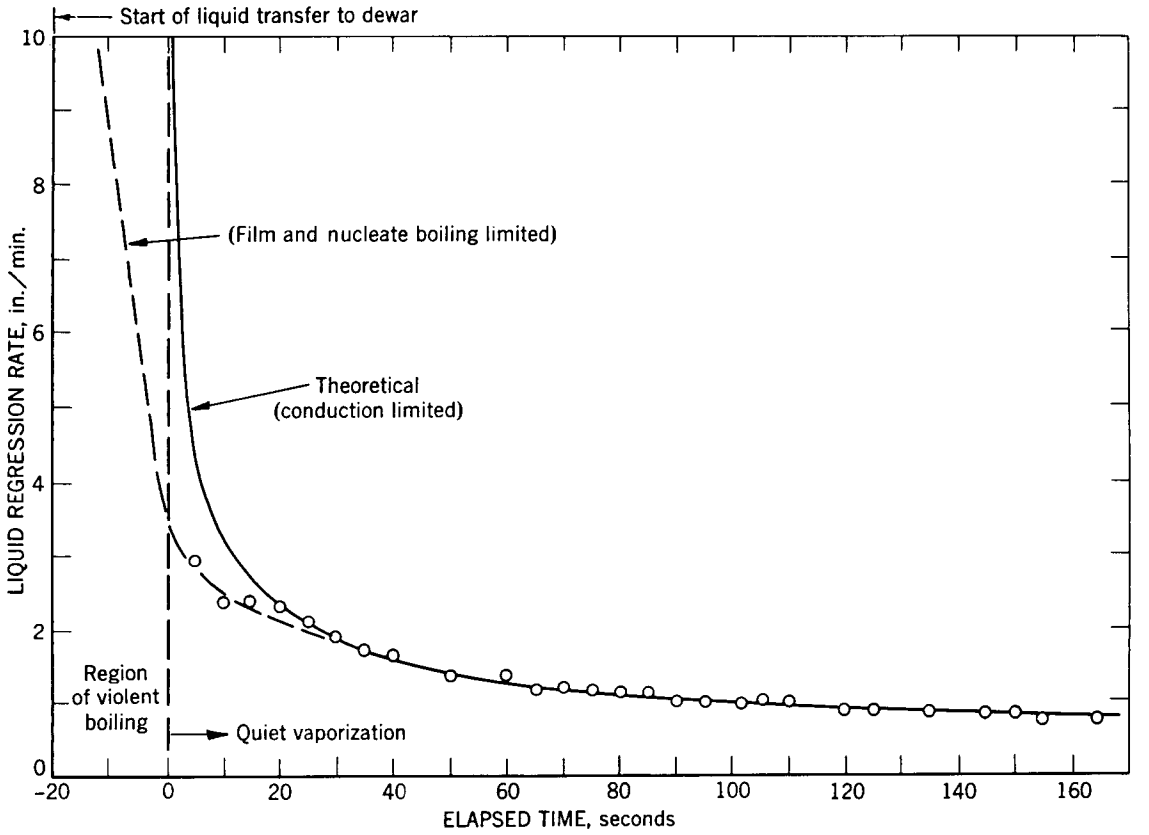

FIGURE 10. - Rate of Vaporization of Liquid Hydrogen From Paraffin in a 2.8-Inch Dewar: Initial Liquid Depth–6.7 Inches.

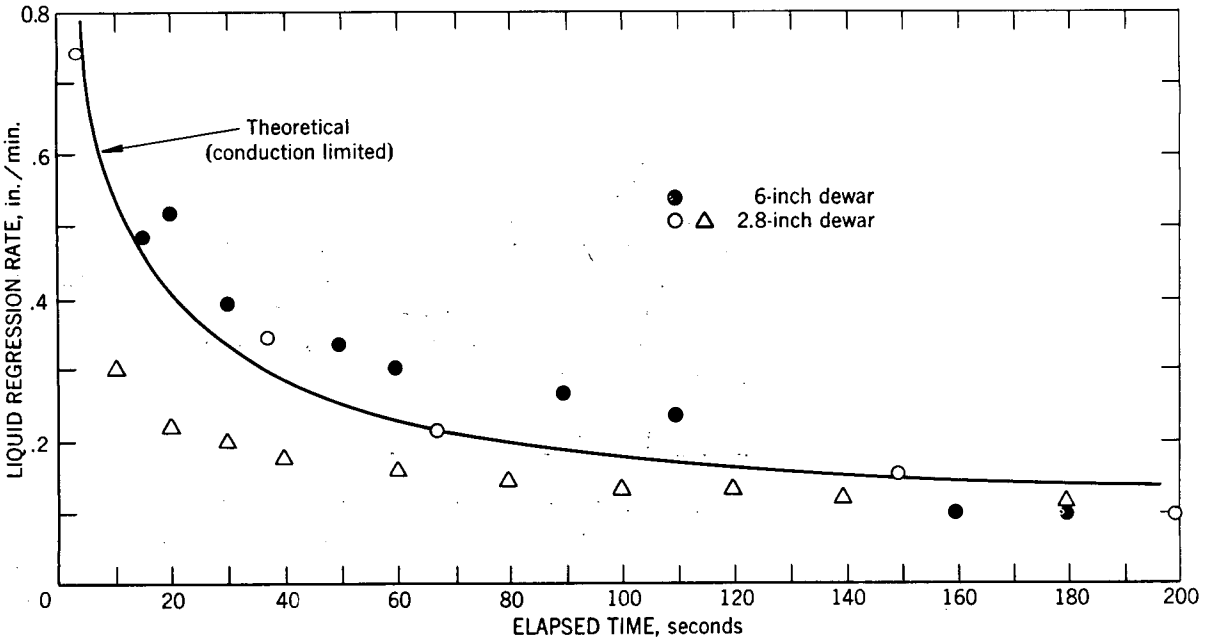

FIGURE 11. - Rate of Vaporization of Liquid Nitrogen From Paraffin in 6-Inch and 2.8-Inch Dewars.

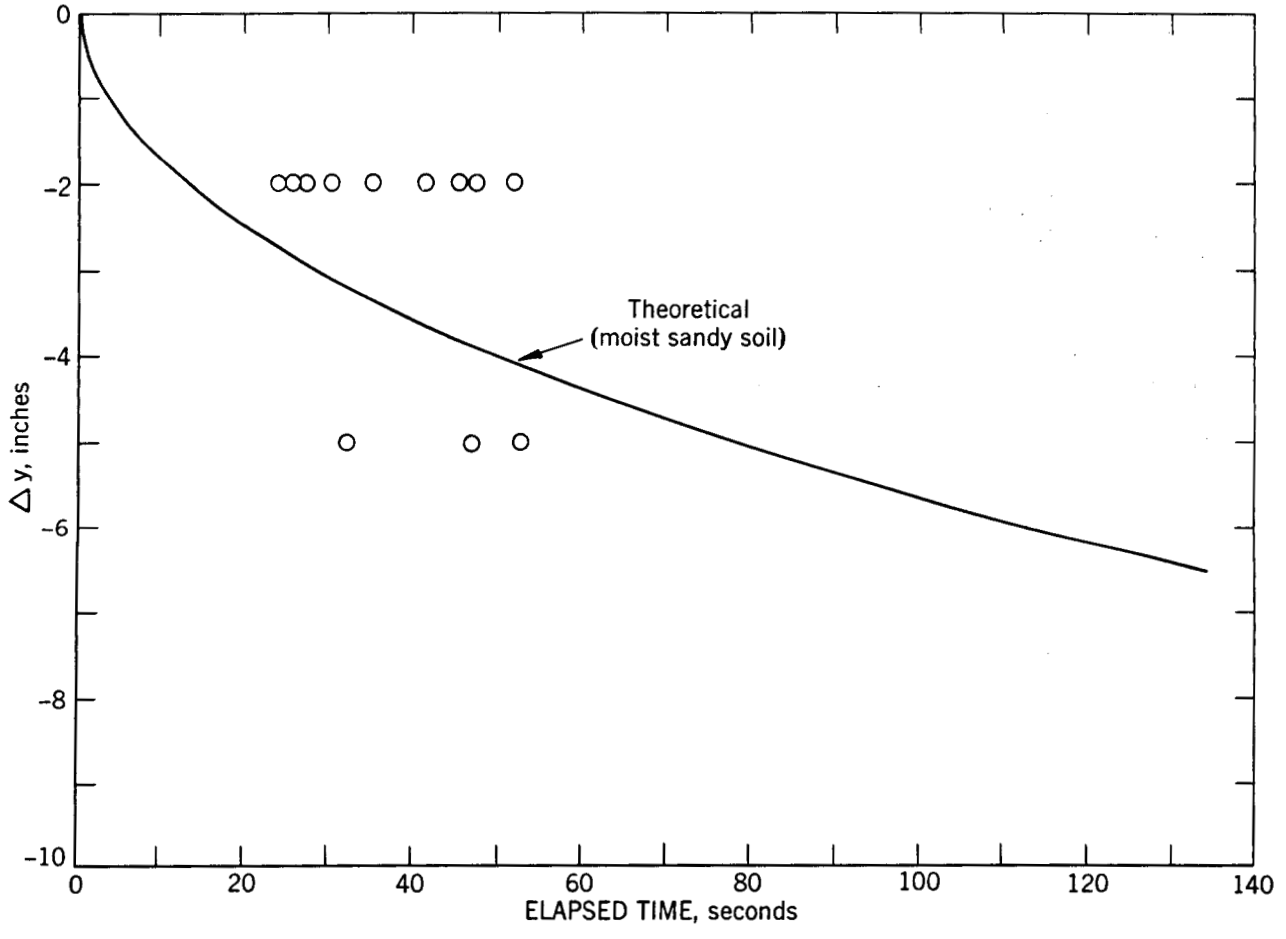

FIGURE 12. - Decrease in Liquid Hydrogen Level Following Spillage in Diked Sandy Area (Data From Ref. 13).

surface and on a four-inch layer of gravel are plotted against the time following spillage; the effect of the high specific surface of gravel is quite marked. Figure 14 shows the positions of the flames produced by the spillage of approximately 56 liters of liquid hydrogen on gravel and smooth steel surfaces. The high specific surface of the gravel causes rapid vaporization of the liquid near the dewar; the center of the base of the flame was much farther from the dewar when vaporizing from a smooth steel plate. Atmospheric conditions were nearly the same in each case.

Mixing of Hydrogen With Air

The spillage of liquid hydrogen into the atmosphere presents a gas explosion hazard because of the rapid vaporization of the hydrogen and the subsequent formation of flammable hydrogen-air mixtures. The volume of free (unenclosed) space rendered flammable in this manner at any time is determined by the rate at which the liquid hydrogen vaporizes and mixes with the surrounding air. The vaporization rate is determined by the spillage rate and the rate at which heat is transferred to the liquid, while the mixing rate is determined

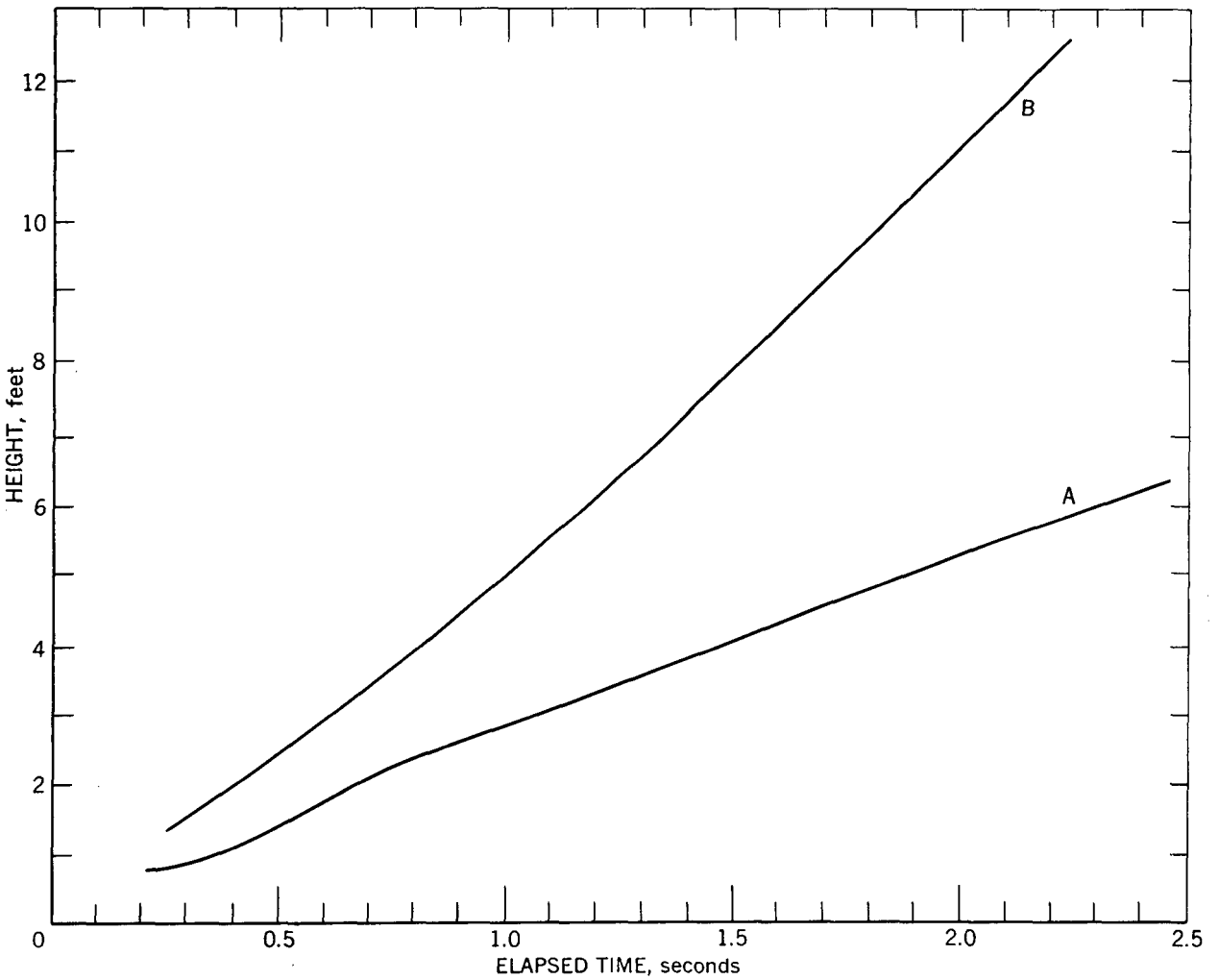

FIGURE 13. - Height of the Visible Clouds Formed After the Rapid Spillage of (A) 6.9 and (B) 6.8 Liters of Liquid Hydrogen at 43° and 36° F., Respectively, on (A) Smooth Macadam and (B) Gravel.

in part by the rates at which heat is transferred to the vapor, and air is brought in contact with it. Since satisfactory estimates of the distribution of the flammable volumes that are formed by the spillage of liquid hydrogen cannot be obtained readily from spillage-, vaporization-, and mixing-rate data, they were determined experimentally with various quantities of liquid hydrogen in the range 0.5 to 7.4 liters. When the liquid was spilled rapidly from open-mouth dewars, it was found to vaporize initially in bursts or pulses and produce very nonuniform vapor-air mixtures above the spill area. Figure 15 gives data that are typical of those obtained in this series of experiments; the hydrogen concentration found in the air at various heights above the spillage plane is plotted as abscissa against the height as ordinate. The hydrogen concentrations obtained at invervals of 2, 4, and 6 seconds following spillage of the liquid are joined by smooth curves. These are used to determine the extent of the flammable mixture compositions; all mixtures containing between 4 and 75 volume percent hydrogen are considered flammable.

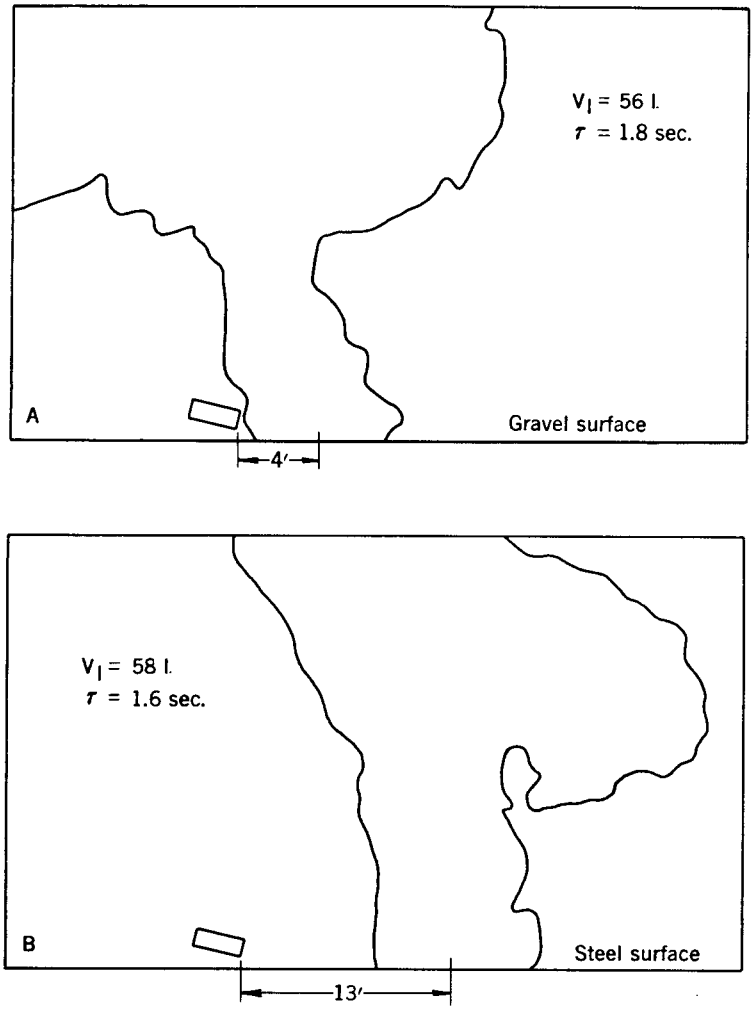

FIGURE 14. - Positions of Flames Above (A) a Gravel and (B) a Steel Plate Spill Area.

Motion pictures were used to correlate the positions of the visible clouds and the flammable spaces that formed after each spill. In general, the visible cloud height was found to be below the height of the upper flammable zone. The difference in heights varied with the relative humidity, air movement, and the time following spillage. This is illustrated in part in figure 16 in which the extent of the flammable mixtures for figure 15 and the height of the corresponding visible cloud are plotted as a function of the elapsed time following spillage.

Figures 15 and 16 illustrate several important points. Since the position of the visible cloud does not coincide with the position of the first flammable mixture zone that is formed following the spillage of liquid hydrogen, the visible cloud cannot be used as a precise measure of the position of the flammable zone. It should be possible to ignite flammable mixtures outside as well as within the visible cloud. On the other hand, since flammable mixtures may not extend to the edge of the visible cloud, it should be possible to pass an electrical discharge within the visible cloud without igniting the hydrogen-air mixtures above a spill area; both phenomena have been observed. Finally, since detached flammable zones exist (figures 15 and 16), a question naturally arises concerning the possibility of flame spread between adjacent detached zones; this is discussed in the following section.

Ignition and Combustion of Hydrogen-Air Mixtures

Ignition of the flammable mixtures above a dewar containing liquid hydrogen produces a momentary yellow flash and then a nonluminous flame. Tests conducted in open-mouth glass dewars often ended abruptly in an orange flash following implosion of the dewar and the subsequent explosive vaporization of the liquid hydrogen. Tests conducted in open-mouth stainless-steel dewars resulted in failure of dewars with soft-soldered rims; as these failed, the rate

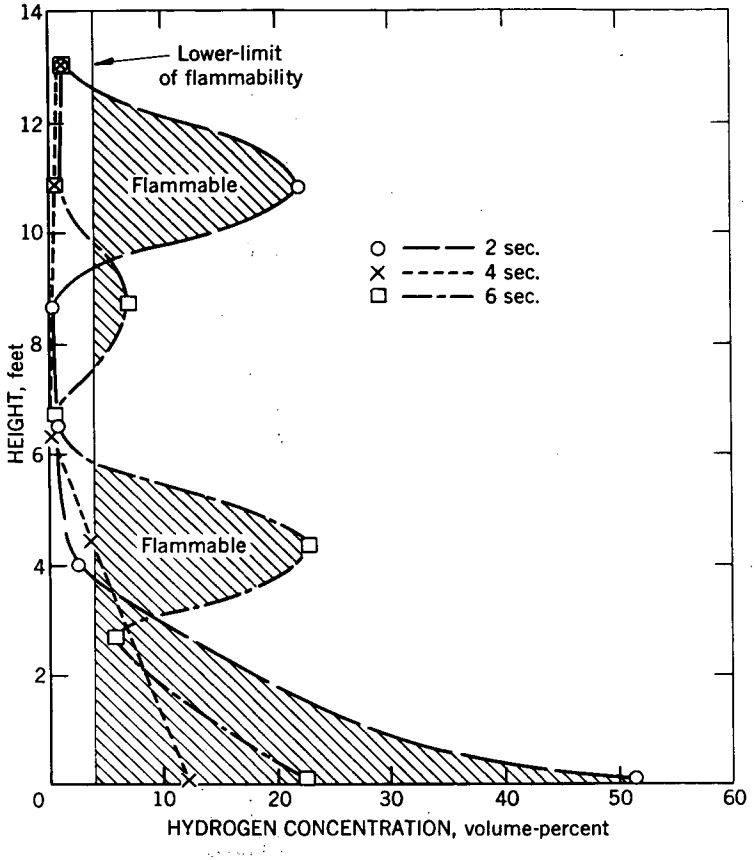

FIGURE 15. - Hydrogen Concentration 2, 4 and 6 Seconds Following the Rapid Spillage of 3 Liters of Liquid Hydrogen on a Dry Macadam Surface in a Quiescent Air Atmosphere at 59° F.

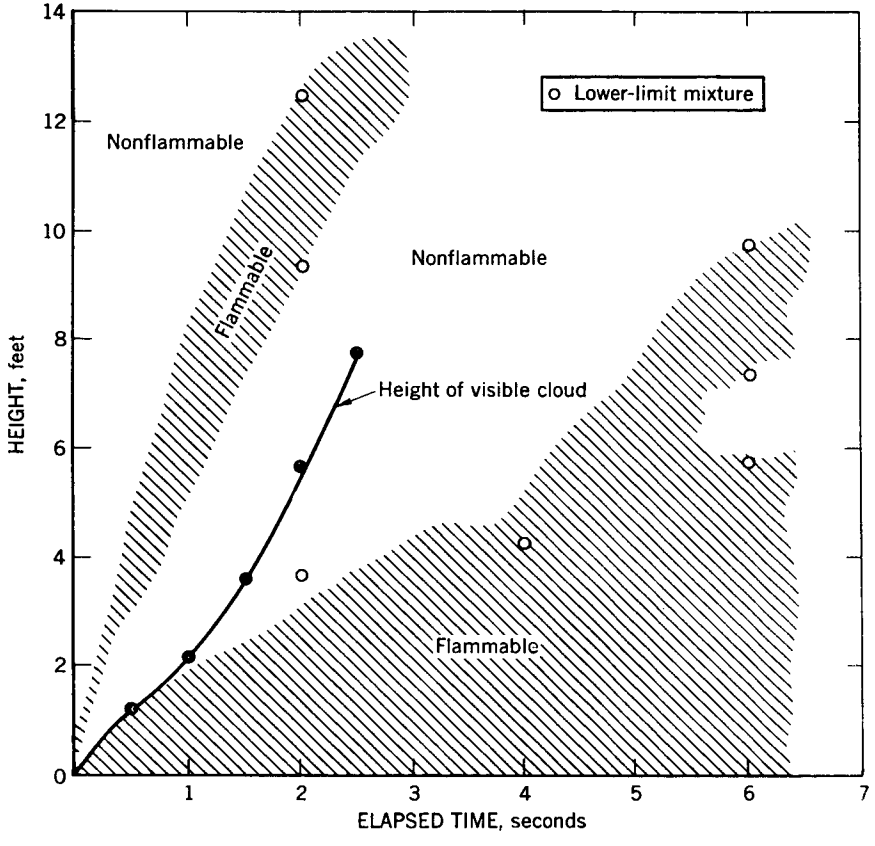

FIGURE 16. - Extent of the Flammable Mixtures and Height of the Visible Cloud Formed After the Rapid Spillage of 3 Liters of Liquid Hydrogen on a Dry Macadam Surface in a Quiescent Air Atmosphere at 59° F.

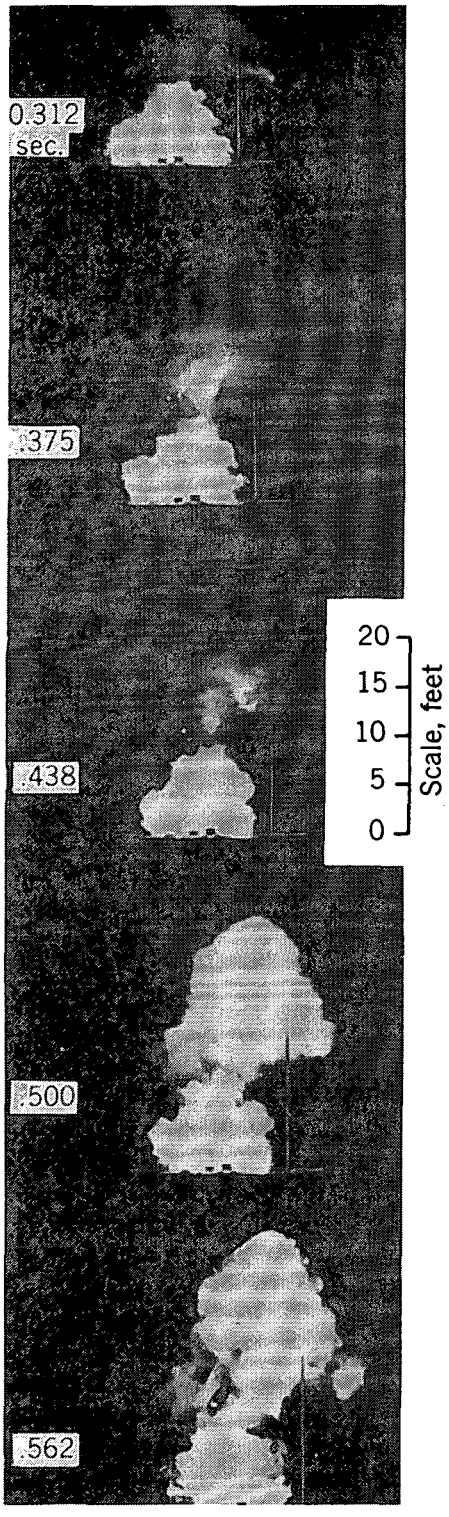

of vaporization of the liquid hydrogen and consequently the flame size increased; near the latter stages, flames extended over the edge and along the outside walls of the dewar. Burning proceeded quietly above stainless-steel dewars with welded rims.

Ignition of the flammable mixtures above a 9-liter dewar followed by spillage of the contents of the dewar produced a burst of flame and rapid burning above the liquid on the ground until the liquid had vaporized.

Ignition of the hydrogen-air mixtures formed in unconfined (open) spaces above a liquid spill area produces rapid-burning flames with dimensions that are dependent on the volume of hydrogen that is spilled, the rate at which it is spilled, the nature of the surface on which spillage occurs, the location of the ignition source, and the time of ignition.

Figure 17 is part of a motion picture sequence that shows the visible clouds and the flames resulting from the rapid spillage of 7.8 liters of liquid hydrogen on a gravel surface 20 inches below an open flame. Several points of interest are evident from this sequence. First, the pulsations discussed in the preceding section are quite evident here. At least two separate flammable volumes were apparently formed. After ignition, the lower volume expanded at about 250 feet per second and ignited the upper volume. An analysis of the complete film strip is given in figure 18.

FIGURE 17. - Motion Picture Sequence (16 frames/second) of the Visible Clouds and Flames Resulting From the Rapid Spillage of 7.8 Liters of Liquid Hydrogen on a Gravel Surface at 65° F. Ignition Source Location: 20 Inches Above Gravel.

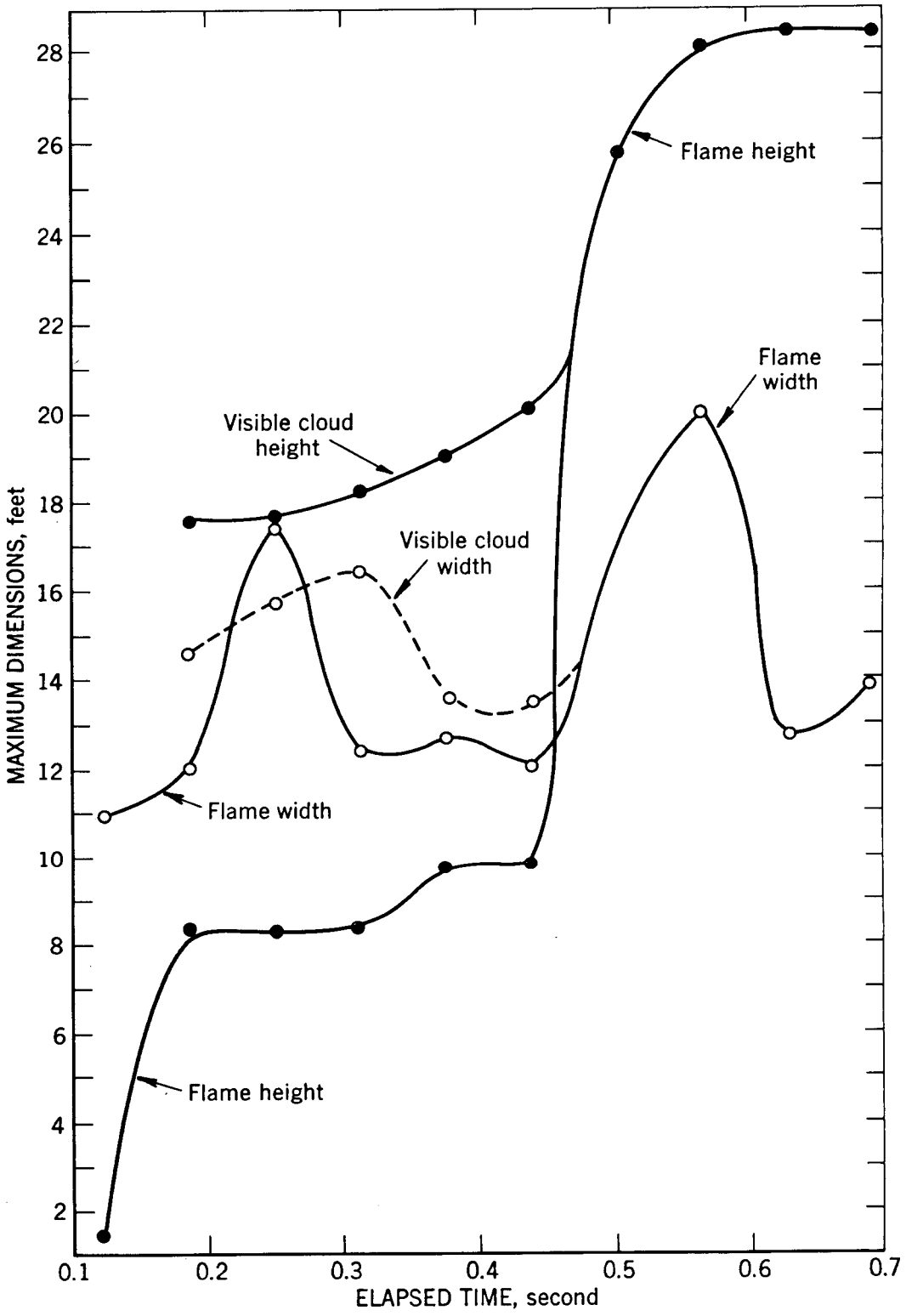

FIGURE 18. - Height and Width of Visible Cloud and Flame Produced by the Rapid Spillage of 7.8 Liters of the Liquid Hydrogen on a Gravel Surface at 65° F., 20 Inches Below an Open Flame.

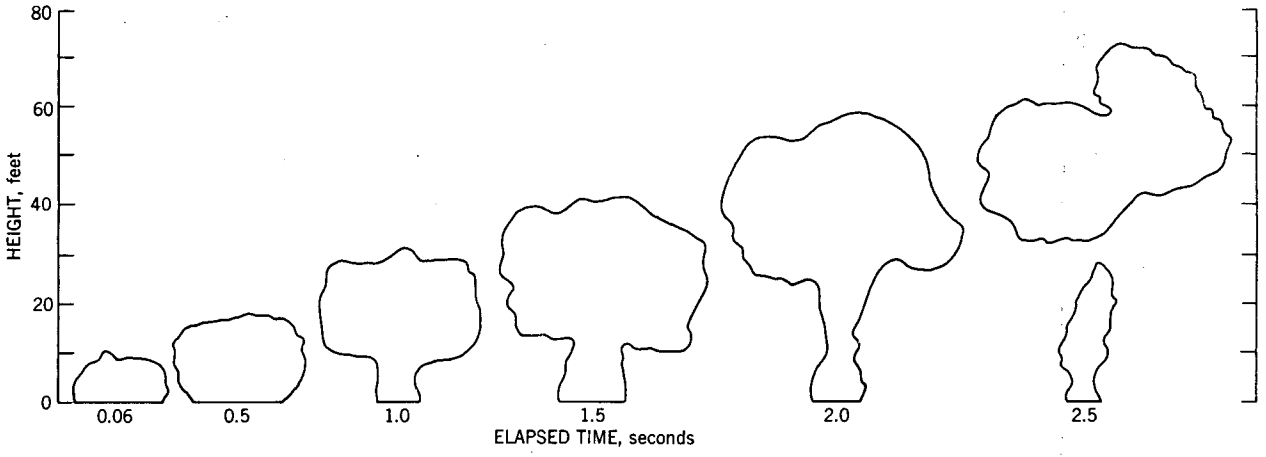

FIGURE 19. - Maximum Vertical Cross-Sections of Flames Produced at Various Time Intervals Following Spillage of 89 Liters of Liquid Hydrogen on a Gravel Surface. (Hor. Scale = Vert. Scale.)

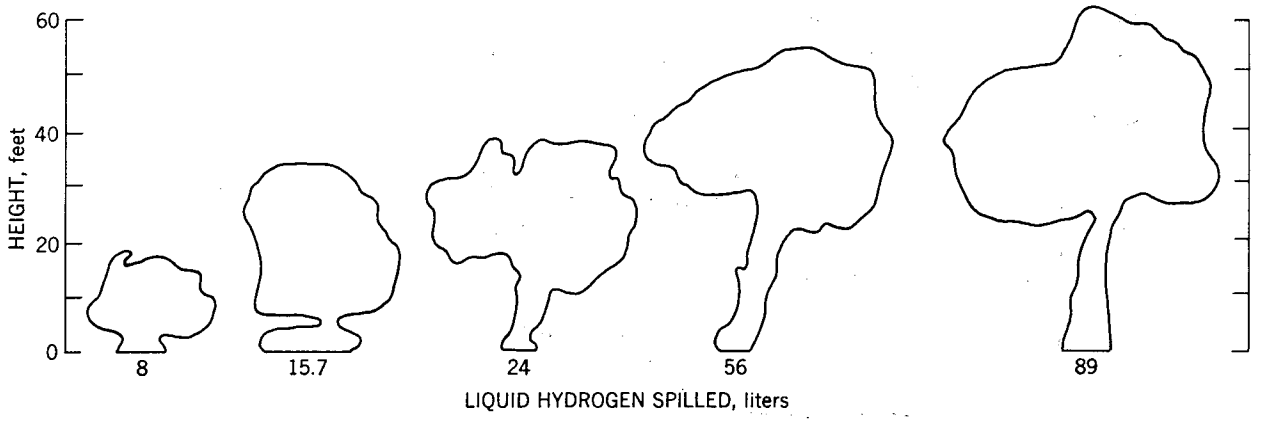

FIGURE 20. - Maximum Vertical Cross-Sections of Flames Produced by the Spillage of 8 to 89 Liters of Liquid Hydrogen. (Hor. Scale = Vert. Scale.)

Detailed studies of the above pulsations showed that detached fireballs are often produced. These float upwards at rates of about 20 feet per second. Figure 19 shows the vertical cross sections, at six time intervals following ignition, of the flames produced by the spillage and ignition of 89 liters of liquid hydrogen on a gravel surface. A detached fireball is shown in the last cross section. Such fireballs usually broke up and disappeared rather quickly. The maximum cross sections attained by flames that resulted from the ignition of the vapors from 8, 15.7, 24, 56 and 89 liters of hydrogen are shown in figure 20. A plot of the maximum height and width attained by such flames prior to breakup is given in figure 21. The data are represented fairly well by the equation

$$H_{max.} = W_{max.} = 7\sqrt{|V_1|} \text{ feet} = 17.8\sqrt{|M|} \text{ feet} \qquad (14)$$

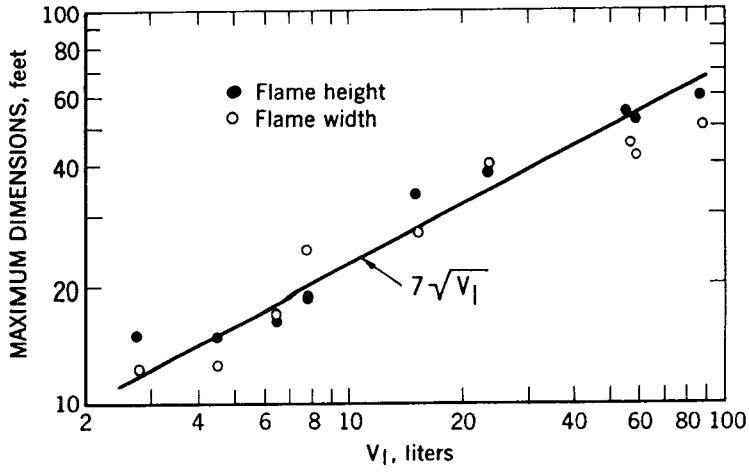

FIGURE 21. - Maximum Flame Height and Width Produced by the Ignition of the Vapor-Air Mixtures Formed by the Sudden Spillage of 2.8 to 89 Liters of Liquid Hydrogen (V_l).

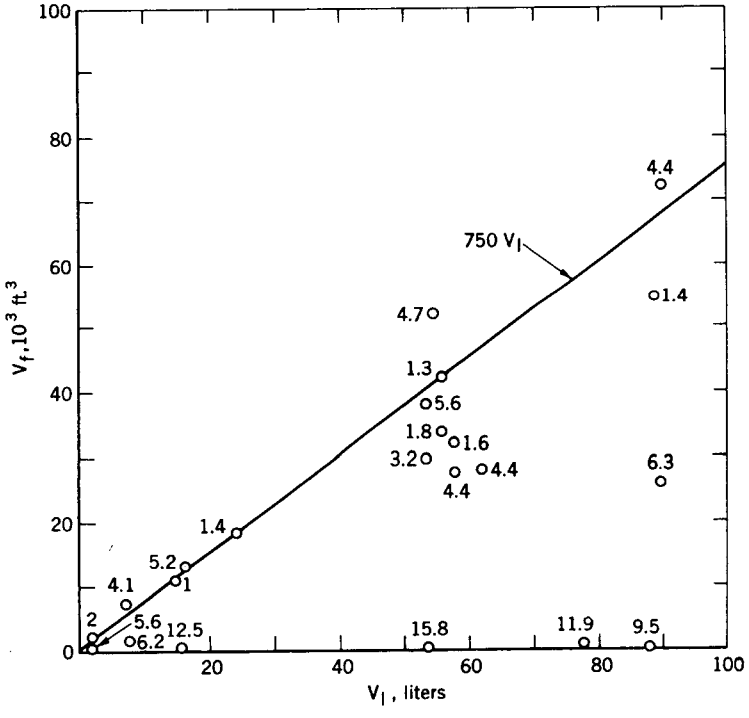

FIGURE 22. - Flame Volumes Produced by the Ignition of the Hydrogen Vapor-Air Mixtures Formed Above Pools of Liquid Hydrogen When Ignited Between 1.0 and 15.8 Seconds After the Spillage of the Liquid Onto a ½-Inch Steel Plate or on 4 to 6 Inches of Loose Gravel.

where $H_{max.}$ and $W_{max.}$ are the maximum flame height and width, respectively, V_l is the volume of liquid hydrogen in liters, and M is the mass of this volume in pounds.

The flame volumes produced by the ignition of the hydrogen-air mixtures formed above the pools of liquid hydrogen (ignition times varying from 0 to 15.8 seconds after spillage of the liquid onto various surfaces) are plotted in figure 22 as ordinates against the corresponding liquid volumes as abscissa. The time between the instant of spillage from an open mouth dewar and the instant of ignition (delay time) is listed opposite each experimental point. The dependence of the flame volume on the delay time is evident from this figure. Under the rapid spillage conditions used here, the maximum flame volume ($V_{f_{max.}}$) is approximately equal to the lower limit mixture volume at 81° F. That is

$$V_{f_{max.}} \approx 750 \; |V_l| \; \text{ft.}^3 \quad (15)$$

where V_l is the liquid volume in liters. Delay times were obtained by the use of an electric timer or the use of open flames placed at various heights above the spillage plane. The former method yielded data that were less erratic since the ignition source (an electric match head) could be placed immediately above the spill area and was not affected by slight gusts of wind. In this method,

the timer was started by a mercury switch mounted directly on the dewar tipping stand. In the latter method, the vapors from an acetone-saturated wick were ignited by the use of a spark plug just before the hydrogen was spilled.

The radiant energy received by one or more surface-type lampblack-coated 12-junction, Bismuth-Silver, Eppley Thermopiles equipped with 1-millimeter-thick CaF_2 windows was recorded with a Model 906A Minneapolis-Honeywell Visicorder.25/ Typical records obtained following the spillage of 5 to 90 liters of hydrogen at ignition delays of 0 to 6.3 seconds are given in figures 23 and 24. These illustrate a number of interesting points. First, the total radiant energy (that is, the area between the radiant-energy curve and the elapsed-time axis) that is produced is determined not only by the quantity of liquid that is spilled but also by the time delay before ignition. The rate of energy release also depends quite markedly on the time delay. Next, the pulses of flammable mixture discussed in this section under "Mixing of Hydrogen With Air" are manifested in some of the radiation records as vibrations. Such vibrations are quite pronounced when ignition delays that are less or greater than the optimum value are employed (curves B and C, figure 23; curve B, figure 24). Finally, since all measurements were made on relatively humid days (about 1 to 2 percent water vapor) a considerable amount of radiation was absorbed in passing through the air. Experiments conducted with steam in 3-1/2-inch and 7-inch cells yielded an absorption coefficient of 0.015/(percent water vapor-foot). The intensity of the collimated radiation from a hydrogen flame is thus given by

$$I = I_o e^{-0.015wr} \qquad (16)$$

where w = percent water vapor

and r = distance in feet.

The radiation flux thus falls off quite rapidly with distance if the air contains as much as 2 percent water vapor; this is less than the saturation value at temperatures above 70° F. at sea level.

The effects of the spillage of the liquid hydrogen and ignition of the vapors on the surroundings can be seen from the thermocouple and thermopile records presented in figure 25. The spillage of 5.4 liters of liquid on a macadam surface causes the surface temperature to drop quickly. Ignition of the vapors at approximately 0.7 second causes the rate of fall in surface temperature to decrease and the air temperature to increase. As is to be expected, the temperatures of all the surroundings increased to values above ambient.

The blast pressures produced by the burning of the vapors above a pool of liquid hydrogen are quite small. Measurements were made both with a General Radio Impact Noise Analyzer and with a Kistler SLM System. Typical overpressure data obtained 160 feet from the ignition source with the noise analyzer

25/ Reference to specific makes or models of equipment is made to facilitate understanding and does not imply indorsement of such devices by the Bureau.

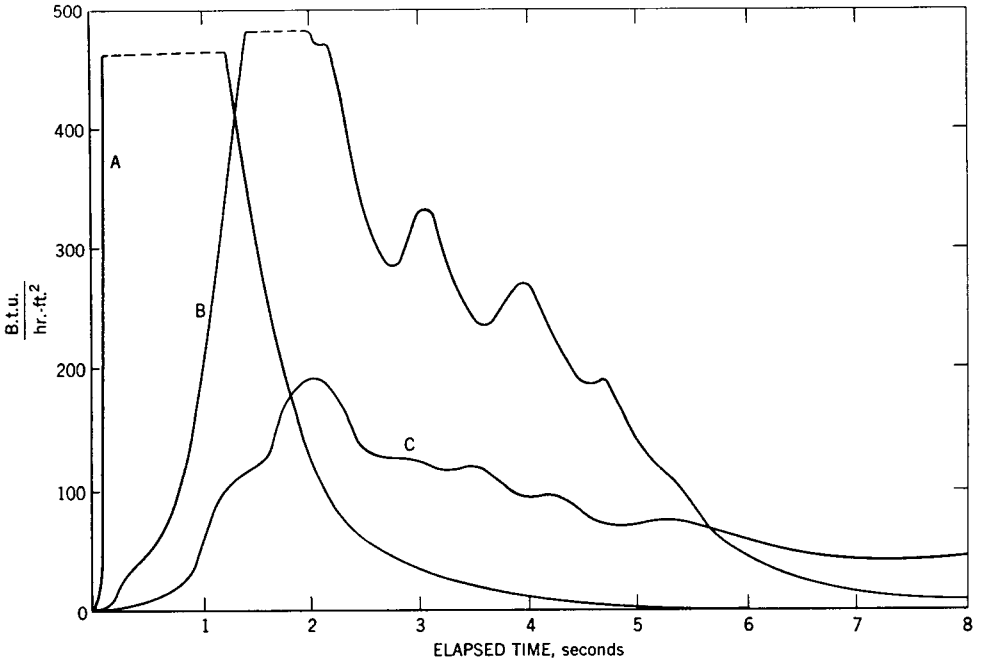

FIGURE 23. - Radiant Energy Received 47.5 Feet From the Ignition Source Following the Spillage of (A) 5.0, (B) 8.0 and (C) 7.4 Liters of Liquid Hydrogen; Ignition Occurred Approximately (A) 1.5, (B) 0.75 and (C) 0 Seconds Following Spillage of Liquid.

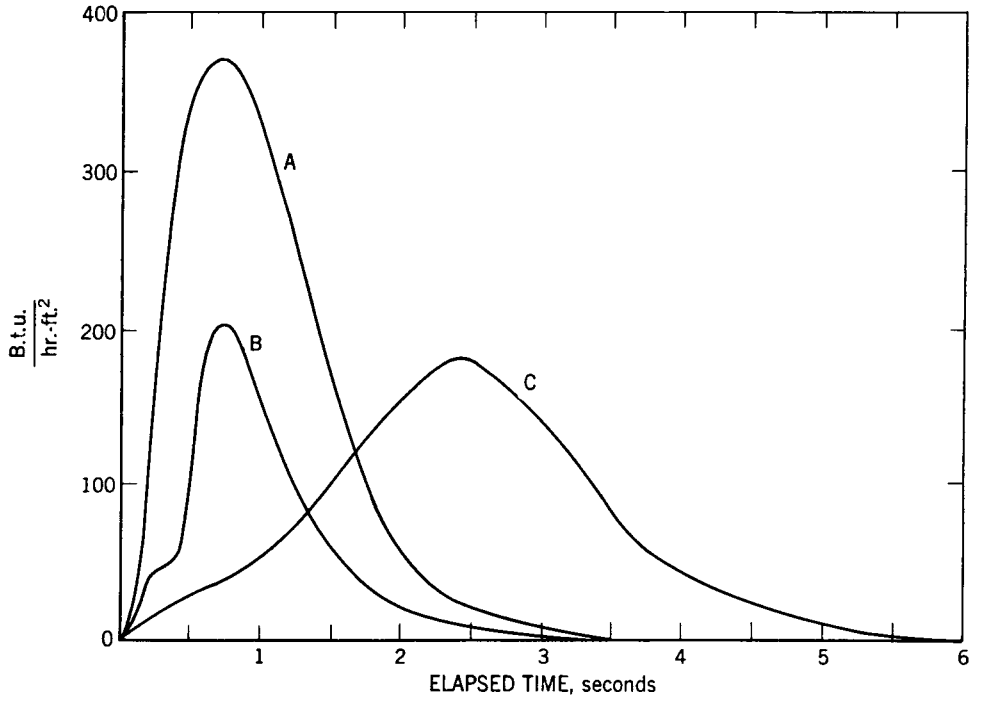

FIGURE 24. - Radiant Energy Received 110 Feet From the Ignition Source Following the Spillage of (A) 90, (B) 90 and (C) 89 Liters of Liquid Hydrogen; Ignition Occurred 4.4, 6.3 and 1.4 Seconds, Respectively, Following Spillage of the Liquid.

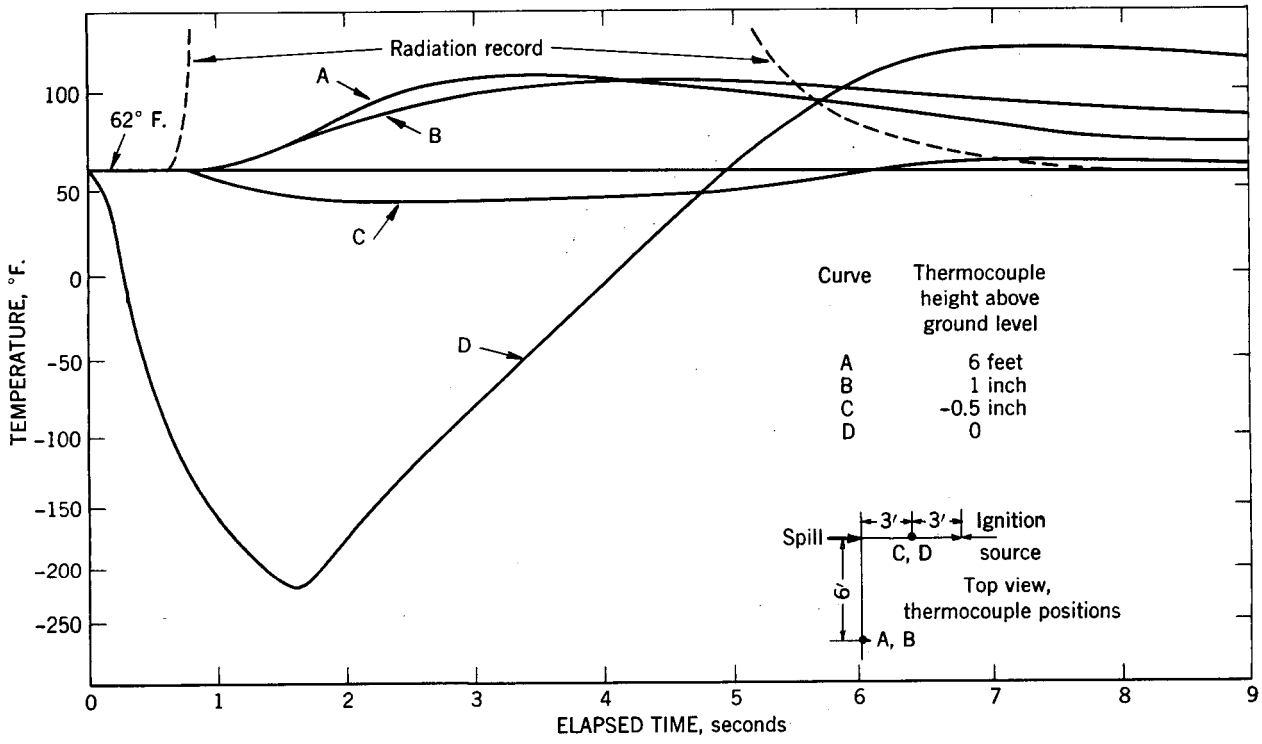

FIGURE 25. - Air and Ground Temperatures Produced by the Rapid Spillage and Ignition of 5.4 Liters of Liquid Hydrogen on a Dry Macadam Surface in a Quiescent Atmosphere at 62° F. (Temperature Measurements With Bare No. 28 Copper-Constantan Thermocouples).

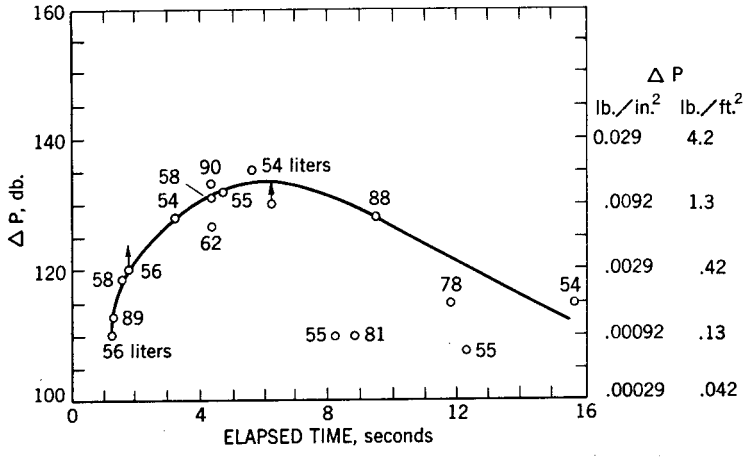

FIGURE 26. - Overpressure (ΔP) Produced at a Distance of 160 Feet by the Ignition of the Hydrogen-Air Mixtures Formed Above Pools of Liquid Hydrogen (54 to 90 Liters as Noted) When Ignited at Various Times (τ) Following Spillage of the Liquid Onto a ½-Inch Steel Plate or on 6 Inches of Loose Gravel.

are given in figure 26. The effect of time delay before ignition is quite pronounced in this figure. The maximum overpressure values obtained at several locations are presented in figure 27. These data indicate that the overpressure is proportional to $1/D^2$ for distances (D) between 80 and 160 feet. In this connection, it is interesting to note that Windes26/ found the overpressure produced by a blast is proportional to $1/D^2$ for overpressures below 0.01 pounds per square inch over distances of

26/ Windes, S. L., Damage From Air Blast: Bureau of Mines Rept. of Investigations 3708, Progress Report 2, June 1943.

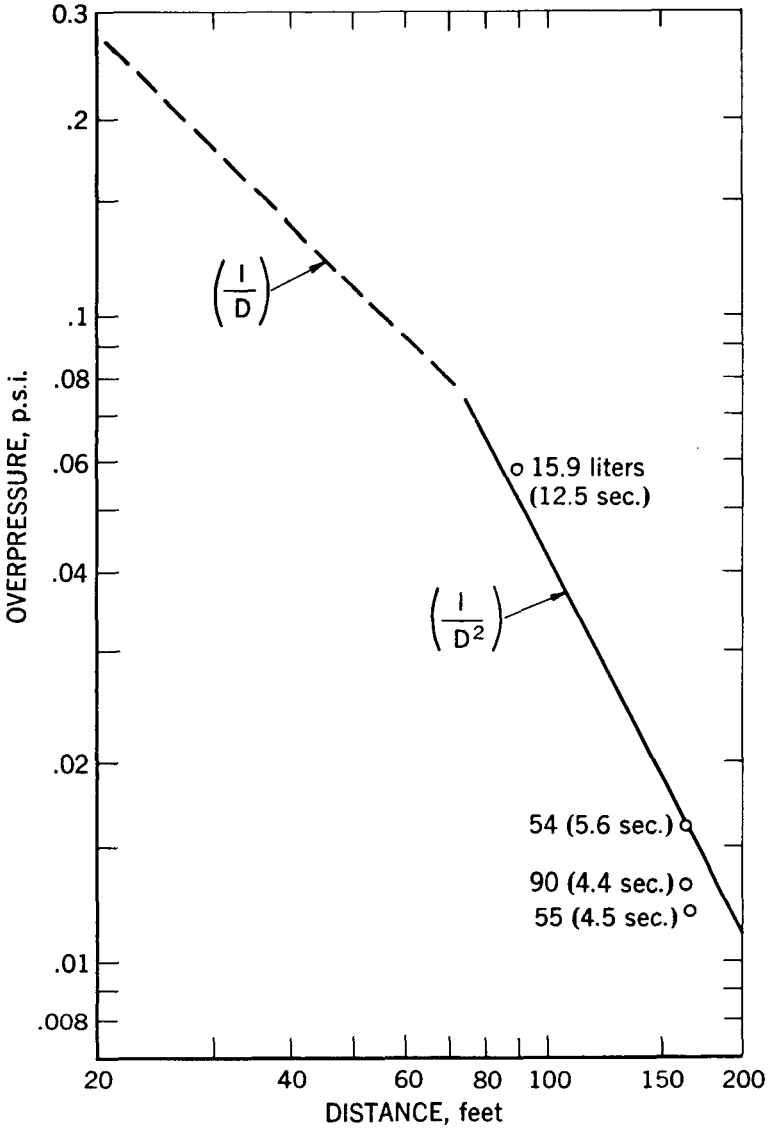

FIGURE 27. - Variation in Maximum Overpressure With Distance Produced by the Ignition of the Hydrogen Vapor-Air Mixtures Formed Above Pools of 15.9 to 90 Liters of Liquid Hydrogen When Ignited Between 4.4 and 12.5 Seconds After Spillage.

approximately 200 to 2,000 feet. At short distances, Ireland[27/] found the overpressure is proportional to 1/D for pressures in excess of approximately 0.1 pounds per square inch. The broken curve in figure 27 gives the overpressure as a function of 1/D.

Burning Above Liquid Pools

Burning Rate as a Function of Time

Flames supported by common fuels are expected to exhibit a "burning-in" period during which a steady temperature gradient is established within the liquid phase. In the case of pure fuels which boil slightly above ambient temperature, this burning-in period extends for 30-40 seconds. At the moment that the liquid surface reaches the boiling point the burning rate approaches a steady value which is maintained as long as the liquid level is maintained constant within the burner. Experimental verification is shown in figure 28 for flames of benzene, ether, and acetone, while methanol and unsymmetrical dimethylhydrazine (UDMH) flames are seen to burn at almost constant rates from the start of the experiment.

We find that methanol and UDMH are exceptional in that radiation from their flames is absorbed very strongly at the liquid surface (see table 3). Also, since radiation is absorbed within the vapor zone above the liquid (see, for example, figure 29), these two fuels are unusual in that conduction and

27/ Ireland, A. T., Design of Air Blast Meter and Calibrating Equipment: Bureau of Mines Tech. Paper 635, 1942.

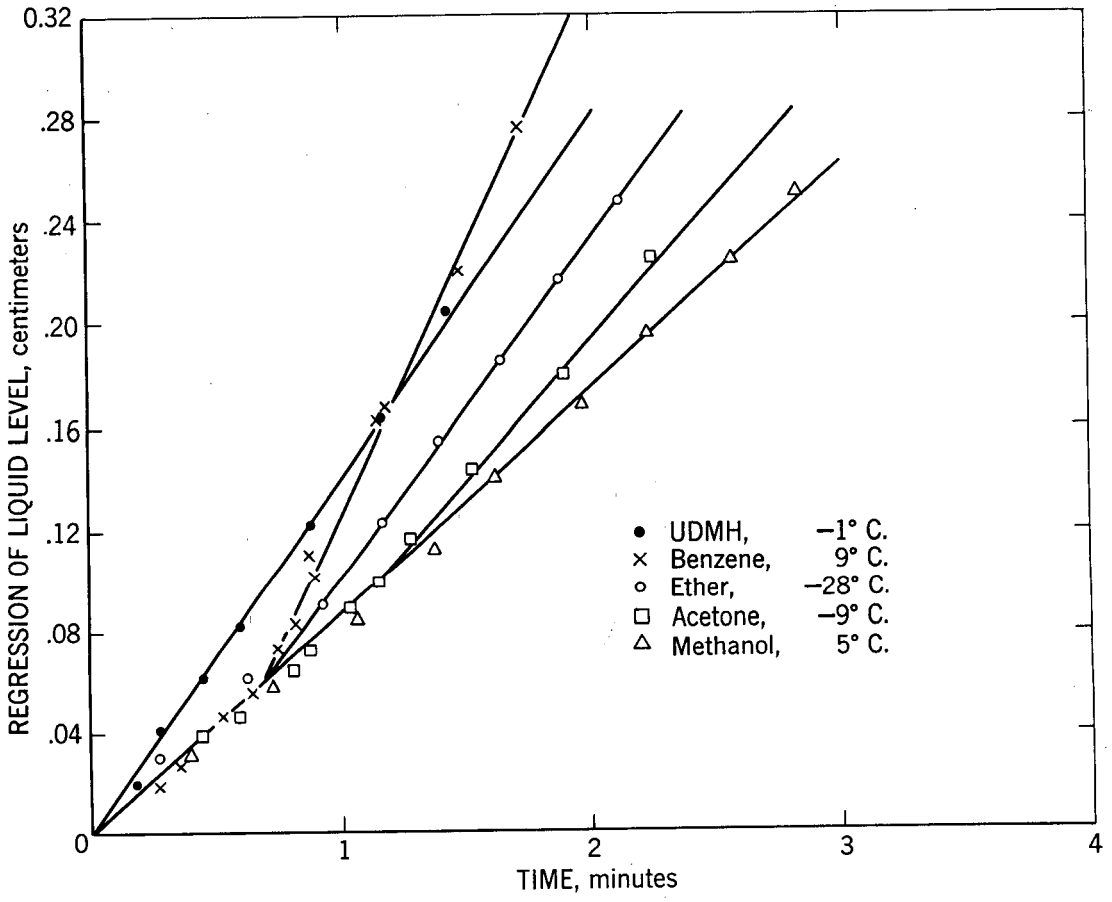

FIGURE 28. - Burning Rates of Five Liquid Fuels in 3-Inch Pyrex Vessel (3.5-inch for UDMH). Vapor Pressure 40 mm. Hg at Initial Liquid Temperature.

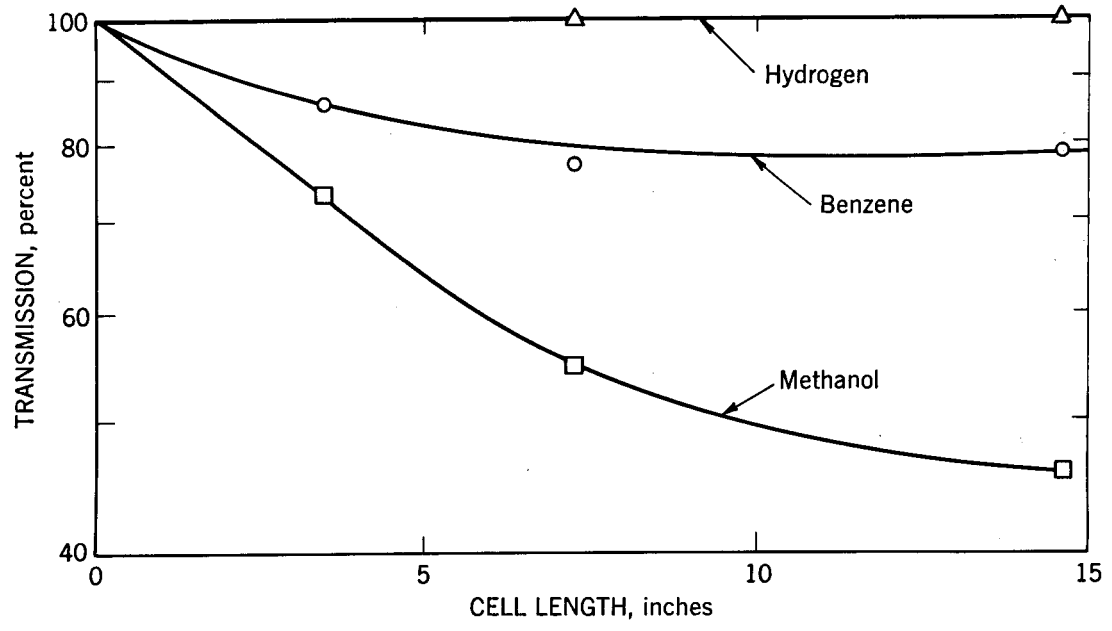

FIGURE 29. - Absorption of Flame Radiations by Fuel Vapors.

convection are relatively important as compared to radiation in heat transport to the liquid. Therefore, the "fast starts" of methanol and UDMH are simply evidence of heat transfer to the liquid surface rather than to the bulk of the liquid. Under comparable circumstances of temperature and vapor pressure, the burning of hydrogen should resemble that of benzene and the common hydrocarbons as regards a burning-in period.

Such circumstances could only exist, however, if the liquid hydrogen were poured onto a very well-insulated surface such as a wide shallow dewar and allowed to reach a steady evaporation rate before ignition. Then the liquid's temperature must be somewhat less than the boiling point (when liquid butane was poured into a 30-inch-diameter tray, its bulk temperature fell from its boiling point of 0° C. to minus 15° to minus 20° C. because of vaporization and, when ignited, its burning rate was low during the first half-minute). But under most conceivable circumstances of spillage, liquid hydrogen would be kept at its boiling point by conductive heat transfer from the ground and a burning-in period should not be encountered. Figure 30 gives the burning rates of liquid hydrogen and of liquid methane at their boiling points in 6-inch dewars. Should ignition of such cryogenic fuels occur within the first minute after spillage, the initial burning rate would undoubtedly be higher, rather than lower, than the steady rate.

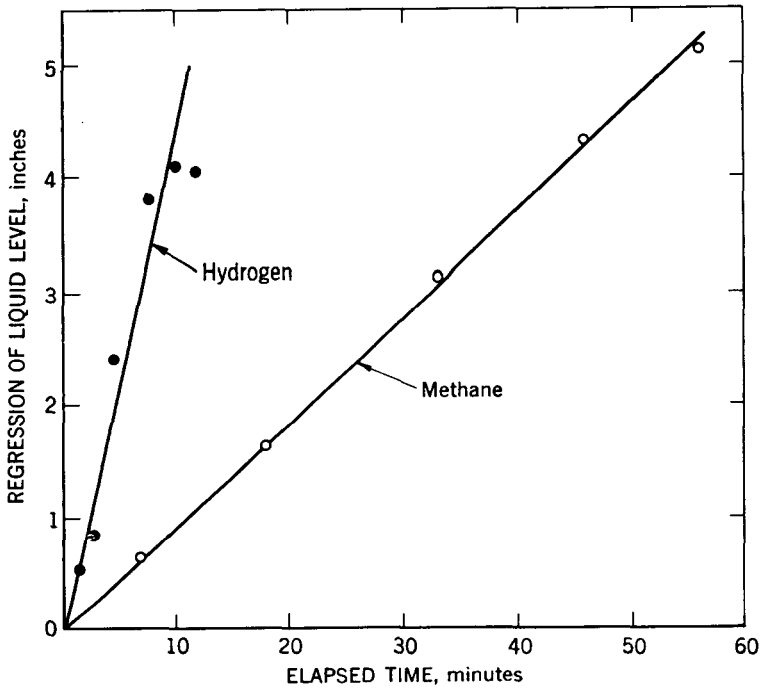

FIGURE 30. - Burning Rates of Liquid Hydrogen and of Liquid Methane at Their Boiling Points in 6-Inch Pyrex Dewars.

Steady Burning Rate as Function of Pool Dimension

The greatest effort in this part of the program was devoted to a test of the principles set forth by Blinov and Khudiakov and by Hottel[28 29/] and to consideration of these ideas as applied to hydrogen burning. An overall test of the Hottel analysis is given in figure 31, in which liquid regression-rate curves calculated from equation (11) and the points representing experimental measurements are given.[30/] It is seen that flames of butane (crosses) and

28/ Work cited in footnote 12.
29/ Work cited in footnote 13.
30/ In equation (11), ρ, T_F, F, and T_B are assumed constant, and K is evaluated from the burning rate at 1-foot diameter relative to the burning rate at very large diameter where $e^{-Kd} \rightarrow 0$. Details of the experimental measurements are given in appendix III.

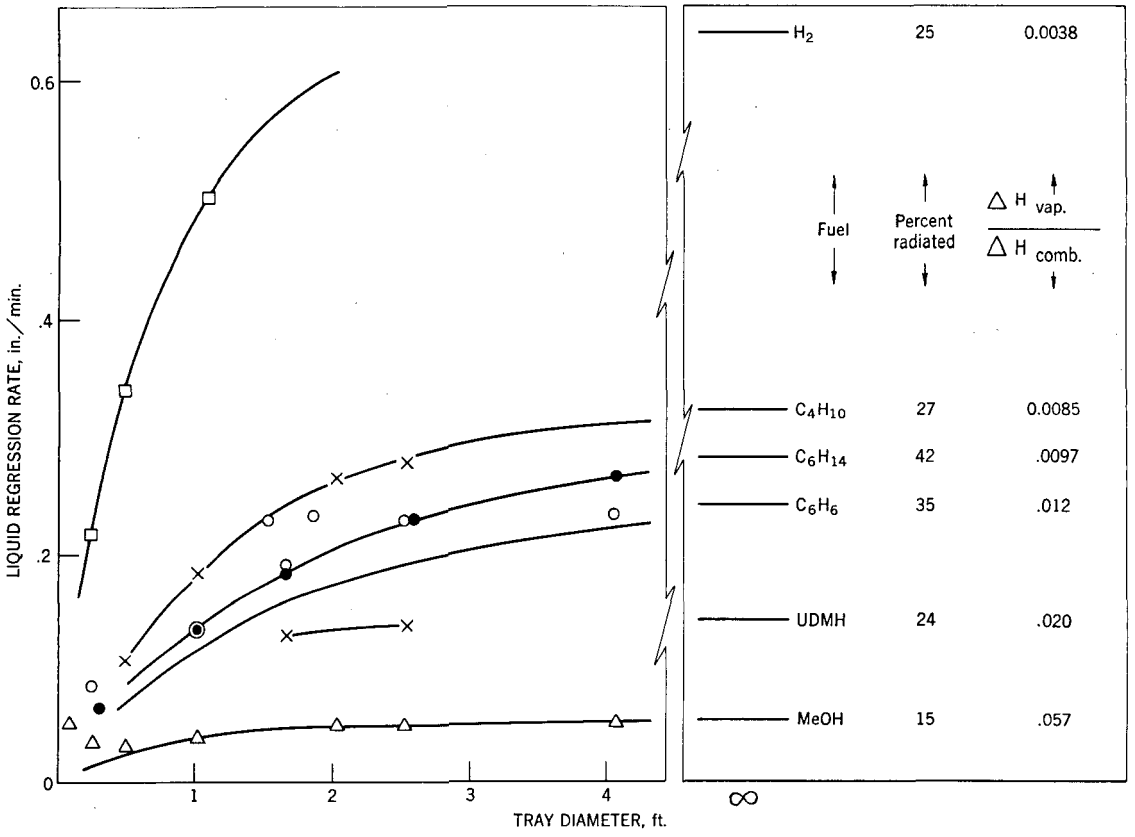

FIGURE 31. - Burning Rates of Liquid Fuels as Correlated by Hottel's Equation, Assuming Radiative Heat Transfer From Flame to Liquid Surface.

hexane (solid dots) are well represented by the Hottel equation, which implies that their mode of heat transfer to the liquid is primarily radiative and that their flame opacities vary in the expected way with tray diameter. Benzene flames (open circles) exhibit a burning-rate plateau such as the one shown in figure 8; this is discussed further as an effect of wind in a subsequent paragraph of this section("Effect of Wind on Burning Rate"). Methanol (triangles) and UDMH (crosses) burning rates are too slightly dependent on tray dimension to provide a test of the theory, but it is clear, nonetheless, that each of these common fuels exhibits a flattening of the curve of burning rate versus tray diameter. In the case of hydrogen, the largest tray (dewar) diameter was 13 inches so that no independent estimate could be made of burning rate at very large diameters. However, the following experimental evidence is appropriate: (1) Since thermocouples in the hydrogen vapor zone between flame and liquid show no sharp increase in temperature as they leave the liquid, heat transfer from the flame to the liquid surface is clearly radiative at even the smallest dewar diameters. (2) The percentage of combustion heat radiated to the surroundings is nearly the same in the 13-inch-diameter dewar (25 percent radiated)[31] as in spillage experiments involving a fireball of 50-foot diameter; therefore, the flame's opacity to its own radiation must reach a maximum in about the same way as in the flames of the common fuels. On the basis of

31/ Compare with David, W. T., and Parkinson, R. M., Radiation in Gaseous Explosions: Phil. Mag. S. 7, 15, No. 96, 1933, pp. 177-192.

these findings, the curve for hydrogen in figure 31 was drawn to best fit the three experimental points; this requires that K have a value of 1.5 feet^{-1} or that e^{-Kd} be effectively zero at a tray diameter, d, of 3 ft. The "limiting" value of burning rate is then of the order of 0.6 inch per minute, although experimental uncertainties in the three measurements plotted could easily have affected this value by as much as 50 percent.32/

Steady Burning Rate as Determined by Fuel Properties

The best available evidence for the correctness of the above burning rate of liquid hydrogen is given in figure 32 wherein the experimental burning rates of six pure fuels are correlated quite successfully with the fraction of the flame's heat of combustion which must be fed back to the liquid to maintain steady vaporization. $\Delta H_{vaporization}$ in this figure is an "effective" latent heat, which includes the integrated heat capacity of the liquid between ambient temperature and the boiling point. All other candidate factors, such as vapor pressure, are successfully ignored. The ordinate of figure 32 refers to burning rates as estimated at very large tray dimensions from figure 31. One can appreciate that such a correlation could not possibly hold if burning rates at small diameters were to be considered. For example, as shown in figure 8, the burning rates of the two hydrocarbon blends are much affected by fuel volatility in trays of small diameters but almost independent of this factor in large trays. Unfortunately, published information on burning rates of other pure fuels almost invariably refers to tray diameters of 1 foot or less and is therefore not useful for further testing of the above correlation. As suggested by the stray point for Blinov and Khudiakov's "aviation gasoline" (solid dot,

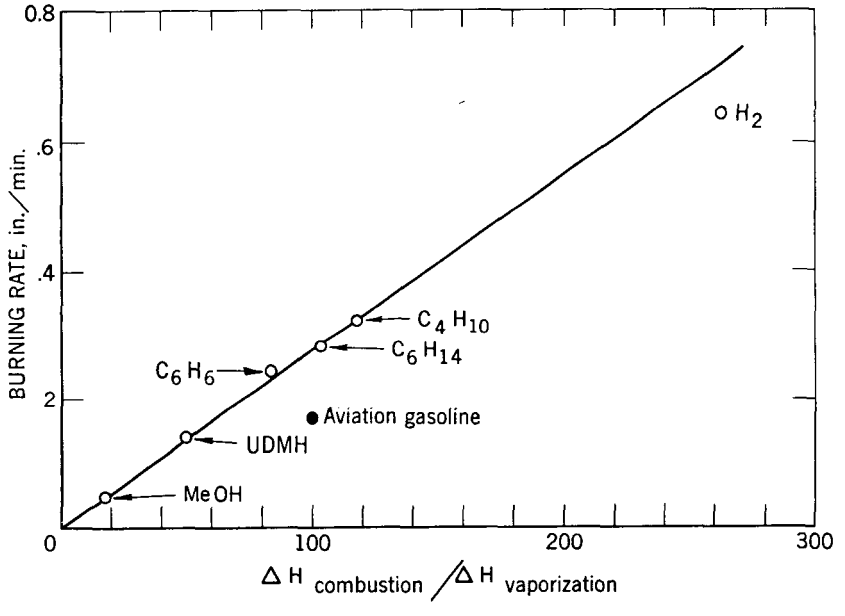

FIGURE 32. - Relationship of Liquid Burning Rates at Large Tray Diameter to Two Physical Properties of Fuel.

32/ The major uncertainty lies in the correction to be made, if any, for heat conduction through the walls of the dewar. As shown in figure 36, when the liquid hydrogen burns down to approach the bottom of the dewar, the burning rate approaches a constant value; in the 6-inch dewar, this hydrogen-loss rate (evaporation rate) is shown to correspond to the normal heat-loss rate of the dewar. We have therefore subtracted the final measured rate at each diameter from the initial burning rate to obtain the points in figure 31. It is by no means certain that the above correction is justified.

figure 32) there is still some uncertainty with regard either to blended fuels or to fuels of high boiling point.

Phenomenological Aspects of Pool-Supported Flames

As we follow the correlation line in figure 32 from methanol to hydrogen, we pass from "short" to "tall" flames, and from periodic to random fluctuations of flame shape, as well as from slow to fast burning. We think that most of the descriptive aspects of the burning are related chiefly to the absorption of the flame's radiation by the fuel vapor and by the liquid fuel. Strong absorption by the vapor requires that the flame stand close to the liquid to vaporize fuel by radiation and also raises the temperature of the vapor zone. Other things being equal, this improves the likelihood that convection will play a role in the transfer of heat (with methanol, UDMH and benzene flames, the liquid level could be located precisely by thermocouples, since there was a sharp temperature discontinuity at the surface; this method was useless with butane and hydrogen flames). Strong absorption of the flame's radiation by the liquid leads to a steep temperature profile in the liquid phase (figure 33), decreases the burning-in period following ignition, and undoubtedly strengthens the coupling between pulses of fuel vaporization and pulsations of heat transfer from the flame. Absorptions of radiation by the liquid and vapor phases are usually closely related.

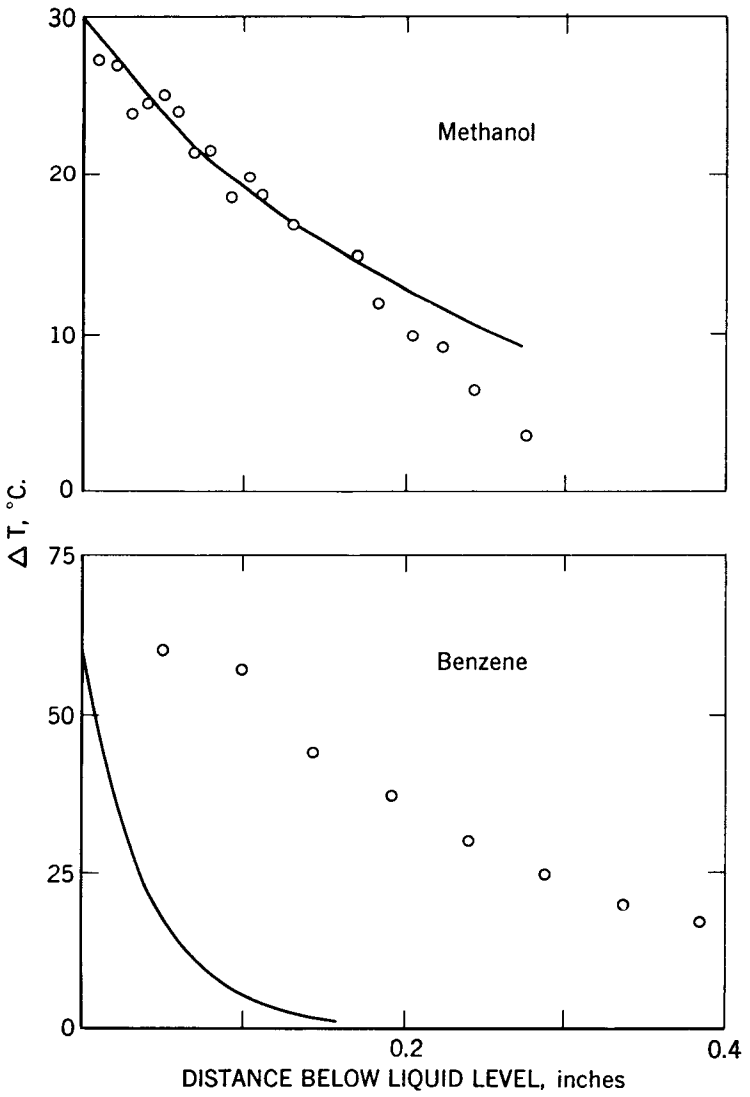

FIGURE 33. - Experimental Temperatures in Liquid Phase Compared With Theoretical Curves for Heat Input at the Liquid Surface. Combustion in 30-Inch Diameter Tray.

The absorption of flame radiation by fuel vapor was measured, using cells of various lengths equipped with calcium fluoride windows. Where necessary the cells were electrically heated to prevent condensation, so that all data refer to gases or vapors at 1 atmosphere partial pressure. Results given in figure 29

indicate that hydrogen flames, despite their nonluminosity, should more nearly resemble benzene than methanol flames in general behavior.

Measurements of absorption of flame radiation by four liquid fuels are given in table 3. No attempt was made to include liquid hydrogen in this comparative study. It is known that liquid hydrogen is very transparent in the infrared, the only excuse for absorption being the weak interactions of quadrupoles. It seems very safe to assume that hydrogen occupies the terminal position in the fuel series with regard to both liquid and vapor phase absorption.

Related to the considerations above are two other qualitative aspects of flame behavior that have been reported. Blinov and Khudiakov[33/] have been much concerned about turbulence in flames of large diameters; for gasoline fires they calculate the Reynolds number of the rising vapor stream to approach 2000-3000 at about the tray diameter with which their burning rates approach a diameter-independent value; this implies that hydrogen, with its low vapor density and high kinematic viscosity, might reach its maximum burning rate only at very large diameters. However, on the basis of our own observations, we have not been able to attach any significance to turbulence in these flames and consider it only as a possible second-order effect.

Another phenomenon that has been considered here is the "creeping" of flames to cover larger ground areas than that of the flame-supporting pool of fuel. This was encountered conspicuously with butane flames at 2-1/2-foot tray diameter and was later simulated in the laboratory with small benzene flames (figure 34). More recently the problem was described by Emmons.[34/] Creeping is more likely when the fuel vapors are dense, that is, when the molecular weight is high and the vapor zone is not heated by absorption of radiation. In the case of hydrogen the low molecular weight seems to outweigh the transparency of the vapor so that flame movement is conspicuously upward.

Effect of Wind on Burning Rate

From inspection of equation (11) it appears that radiation from the flame to the liquid surface can be augmented by (1) an increase in shape factor, F; (2) an increase in flame temperature, T_F; or (3) an increase in the opacity coefficient, K. It is easiest to demonstrate the effect of wind on the last of these factors, the flame opacity, since hydrocarbon flames are extremely sensitive in this regard, and therefore the influence of wind has probably been overemphasized in the literature on open flames.

When a slight draft is imposed on a small benzene or hexane flame, the luminous surface is ruffled and the burning rate is immediately increased (table 4). This is consistent with an increase in $(1 - e^{-Kd})$ of equation (11). By placing a chimney over the flame, as shown in figure 35(B), the burning

---

33/ See footnote 12.

34/ Emmons, H., Some Observations on Pool Burning: Presented at First Symposium on Fire Research, Washington, D.C., November 9-10, 1959.

rate can be increased to its limiting (large-diameter) value, consistent with $(1 - e^{-Kd})$ approaching unity. In figure 31, the points for benzene at 46-centimeter and 56-centimeter diameter (open circles) were obtained by burning benzene in steel drums rather than in flat trays; the resultant upward component of the convection currents evidently played the part of a chimney-induced draft; note specifically that the burning rates were raised almost exactly to the limiting value.

Significantly, one cannot make small flames exceed the large diameter burning rate except by imposing such a draft that the flame surface is torn from the rim of the tray as in figure 35(C). Then the burning rate is increased further, but this is caused by an increase in T_F as the incident air is premixed with fuel vapor (notice the bright zone near the axis of the flame in figure 35(C)). It is hard to imagine such tearing of the flame and premixing of air and vapor under conditions of wind or of natural convection above a spill zone unless there is some sort of bluff body, such as the rim of a tray, to serve as a flame stabilizer.

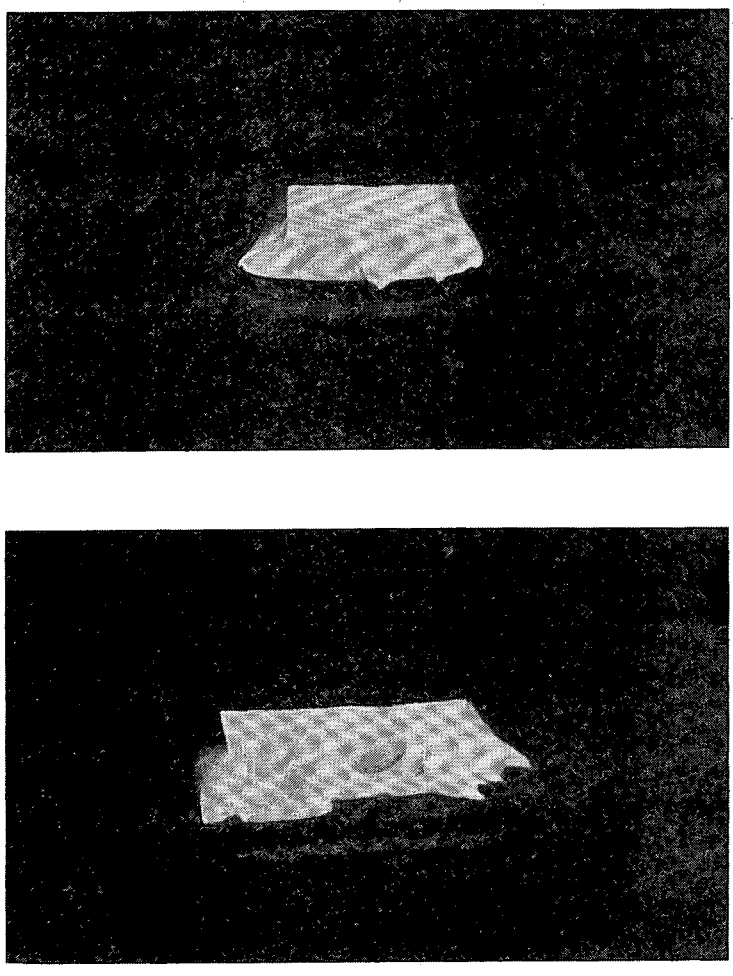

FIGURE 34. - Creeping Flame on Lipless Dish (below) Compared With Noncreeping Flame on Dish With ½-Inch Lip.

The only instance in which we have knowingly encountered an increase in shape factor has been with the "creeping" flames of butane. With these the burning rate reached transient values which were perhaps 20 percent larger than the extrapolated large diameter value of 0.32 inch per minute. However, this is a phenomenon which probably has no significance in hydrogen burning.

The conclusion from this work on the effect of wind is that the linear consumption rate of liquid fuel in large fires, and the total heat to be dissipated, can hardly be very much affected by wind. This was an agreeably surprising result; however, crosscurrents can surely increase the

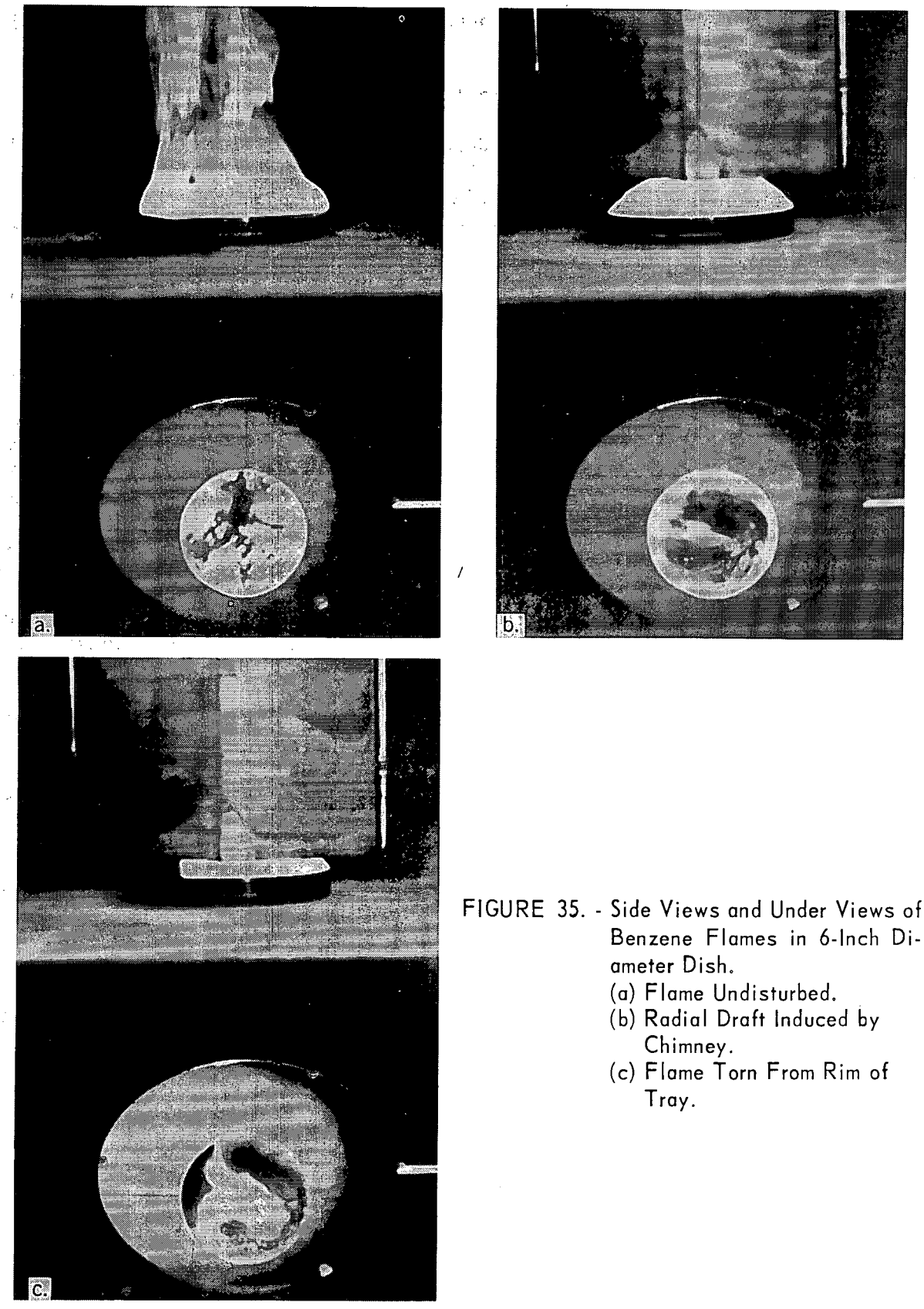

FIGURE 35. - Side Views and Under Views of Benzene Flames in 6-Inch Diameter Dish.
(a) Flame Undisturbed.
(b) Radial Draft Induced by Chimney.
(c) Flame Torn From Rim of Tray.

hazard of a fire's spreading; there appears to be no good way of alleviating this problem.

Radiation From Liquid-Supported Flames

Two distinct problems were considered in regard to flame radiation: (1) That radiation from the reaction zone to the liquid surface must affect the liquid vaporization rate; (2) that radiation from the flame to its surroundings must determine minimum distances for safety of personnel and for storage of combustibles.

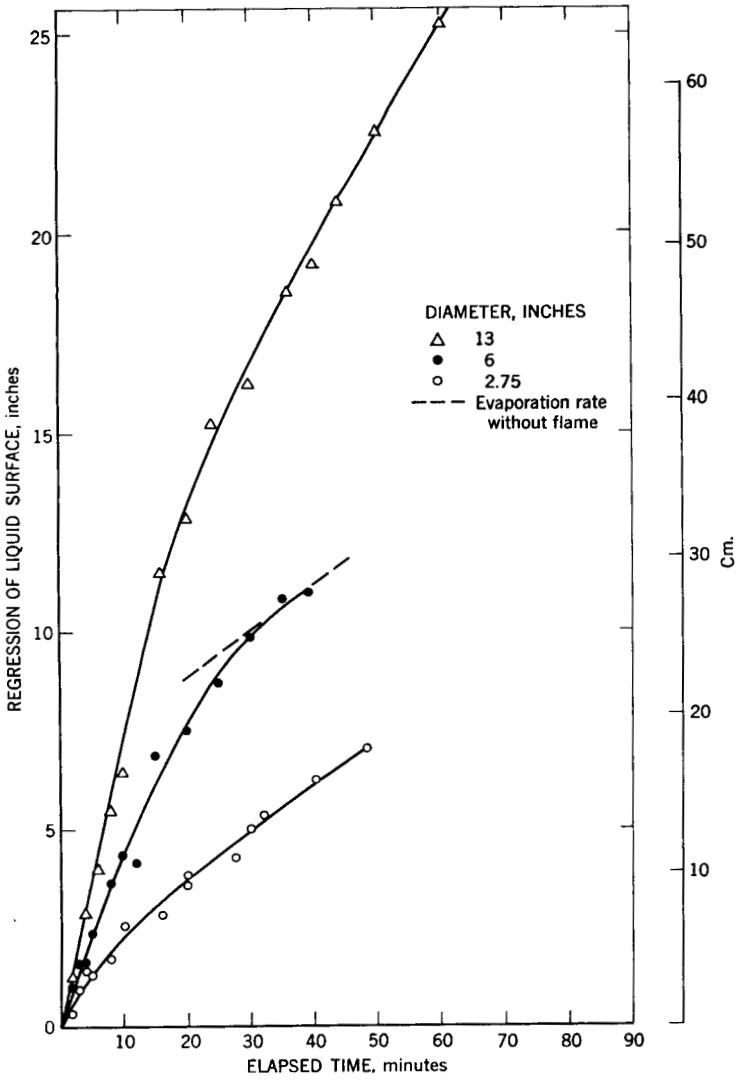

FIGURE 36. - Burning of Liquid Hydrogen in Dewars of Three Diameters (Reconstructed From Flame Radiation Data).

Measurements of radiation to the liquid surface were overemphasized in early stages of the work because hydrogen flames were expected to be analogous to methanol flames, both being nearly nonluminous. This expectation was disproved when temperature measurements were made in the vapor zone above the liquid surface. It then became apparent that heat transfer must be almost exclusively radiative in hydrogen fires but largely convective in methanol fires. The instrument developed for measuring radiation to the liquid surface is described in appendix III. Some preliminary measurements of radiative heat transfer with this instrument are given in table 5. Since the overall heat transfer rate with methanol flames at 1-foot tray diameter was 1.2 watts per square centimeter, the indicated fraction of transfer by radiation was about one-fourth. When it was realized from thermocouple data that hydrogen vaporization could only be radiatively supported, conduction and convection from the flame zone being negligible, this course of study was abandoned.

As discussed above under "Definitions and Theory"

("Radiation From Hydrogen Flames"), one expects the percentage of total heat that is radiated outward from a flame to increase to a maximum as the diameter of the flame is increased. This was tested first with a number of gaseous diffusion flames with the results given in table 6. These results were the first indication here of the unexpectedly large fraction of heat that can be radiated by a hydrogen flame. They also permitted a calculation of the flame's average emissivity based on a photographic estimate of the size of the gaseous diffusion flame on the 16-inch burner. As shown in table 7, the calculated emissivity depends on the assumed flame temperature; from the experimental percentage of heat radiated, one would expect T_F to be about 1,900° K. so that the average emissivity appears to be about 0.01.

The percentages of heat radiated from liquid-supported flames in table 8 are comparable to values obtained with gaseous diffusion flames. Percentages radiated were found to increase quite uniformly with tray diameter if a correction was made, in the case of methanol burning in a 48-inch tray, for absorption of flame radiation by atmospheric moisture. This correction was neglected for the hydrogen flames represented in table 8, since the measuring instruments were located within 10 feet of the flame. However, the atmospheric absorption of radiation from a hydrogen flame is an important safety factor as noted previously in this section under "The Ignition and Combustion of Hydrogen-Air Mixtures." It is worth noting in this connection (table 9) that such radiation absorption is far less favorable in the case of fires involving conventional fuels than of fires involving hydrogen.

CONCLUSIONS AND RECOMMENDATIONS

The chief hazards associated with the use of liquid hydrogen in unconfined (open) spaces are those attributed to:

A. The formation of shock-sensitive condensed (liquid hydrogen-solid oxygen) mixtures.

B. Fire.

The first hazard can be eliminated by excluding oxygen from all systems with which liquid hydrogen comes in contact. The most obvious solution is to flush such systems with an inert gas such as nitrogen or helium. However, since trace quantities of oxygen are difficult to remove from the hydrogen gas to be liquified, solid oxygen deposits may be built up over a period of time in storage containers from which liquid hydrogen is withdrawn periodically; it may be necessary to clean such containers periodically. The second hazard can be minimized by the judicious placement of vent stacks, combustibles, equipment, and buildings. In general, because of the wide range of mixture compositions over which flammable hydrogen-air mixtures can be formed and the high burning velocities of such mixtures, flare stacks should not be used to dispose of excess hydrogen. The current quantity-distance table[35] used for the storage of liquid hydrogen is very conservative. The distances in this

---

35/ Ordnance Corps, Department of the Army, Ordnance Safety Manual: ORDM 7-224, (1951), Sec. 17, 15 May 1958.

table can be decreased safely in all cases in which the formation of shock-sensitive mixtures is precluded. Based on the radiation and flame-size data obtained in the present study, a new quantity-distance table has been constructed as follows:

Distance to inhabited buildings. Assuming all the liquid hydrogen in a container can be spilled and vaporized quickly to form flammable mixtures with air that can be ignited and burned in less than 10 seconds (this would simulate the burning experiments described in this report), the distance r at which we would expect to receive approximately 2 calories per square centimeter (cal./cm.^{2})(This is roughly the radiant flux required to produce flesh burns and ignite certain combustible materials in short exposure times.)[36/] during this short burning period is

$$r_{2\ \text{cal./cm.}^2} = 26 \sqrt{\eta \frac{I}{I_o} |M|} \text{ ft.} \tag{17}$$

where η is the ratio of the radiant energy liberated during burning to the total available energy,

$$\frac{I}{I_o} = e^{-0.015wr}, \tag{18}$$

and M is the mass of the spilled liquid in pounds. If we take η to be 0.3 (that is, 30 percent of the total available energy is radiated during burning) then we have

$$r_{2\ \text{cal./cm.}^2} = 14.2 \sqrt{\frac{I}{I_o} |M|} . \tag{19}$$

A plot of $r_{2\ \text{cal./cm.}^2}$ is given in figure 37 for w = 0, 1 and 2 percent water vapor and for M between 10 and 10^5 pounds of hydrogen. The effect of even small quantities of water vapor is seen to be quite pronounced. Considering the assumptions that were made, the values of $r_{2\ \text{cal./cm.}^2}$ for a water vapor concentration of 1 percent should be quite conservative for use in establishing a suitable table of distances. These values were used to compile table 10.

If the liquid hydrogen in a container is not spilled and vaporized quickly, the above analysis is not entirely applicable. In such a case, the total flux needed to produce second degree burns in 50 percent of the personnel that are exposed is reportedly given by the expression:[37/]

$$Q_c = 3.56 \ |t|^{0.196} \text{ cal./cm.}^2 \tag{20}$$

where t is the exposure time in seconds.

36/ Glasstone, S., The Effects of Nuclear Weapons: U.S. Atomic Energy Commission, June 1957, pp. 296-308.

37/ See footnote 24.

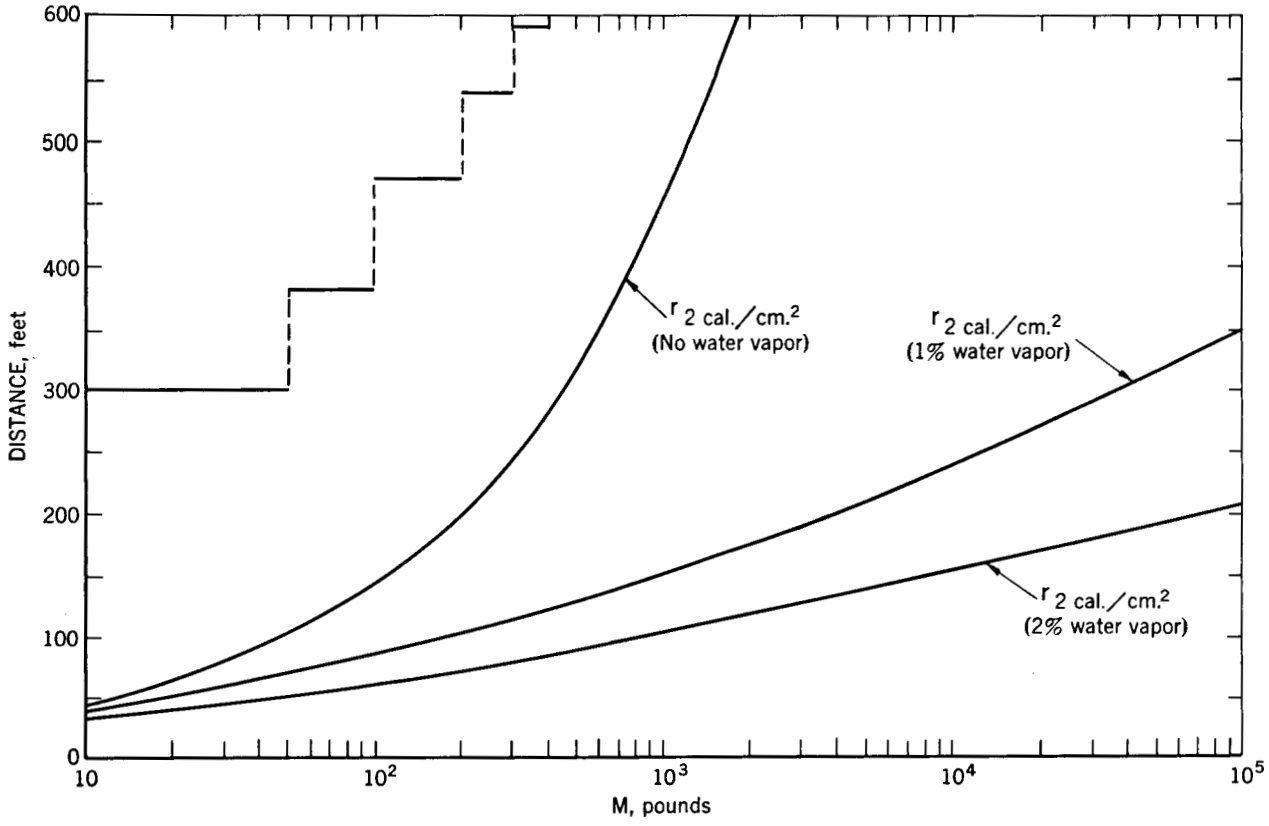

FIGURE 37. - Variation in Distance to Unbarricaded Inhabited Buildings (Class 950 Materials) and $r_{2\ cal./cm.^2}$ With Mass (M) of Liquid Hydrogen.

If we again take η to be 0.3, then for dry sandy soil, with no water vapor present in the air

$$M = 0.0856 \sqrt{t}\,|A| \quad \text{lbs.}\underline{38/} \tag{21}$$

$$\text{and } r_{Q_c} = 3.1 \sqrt{A}\,|t|^{.152} \text{ ft.} \tag{22}$$

$$\text{or } r_{Q_c} = 3.9\,|M|^{0.304}\,|A|^{0.196} \text{ ft.} \tag{23}$$

Where M is the quantity of liquid that is burned in t seconds from a pool of area A ft.^{2}.

If we take

$$A = \frac{|M|}{2 \log_{10} |M|} \text{ ft.}^2 \tag{24}$$

38/ $M = 0.149 \sqrt{t}\,|A|$ lbs. for moist sandy soil.

then

$$r_{Q_c} = \frac{3.9\sqrt{|M|}}{(2 \log_{10} |M|)^{.196}} \text{ ft.} \quad (25)$$

Equation (25 yields distances to inhabited buildings that are smaller than those listed in table 10A for hydrogen quantities below approximately 10,000 pounds but larger than those listed in this table for quantities above approximately 10,000 pounds. Again, if a small amount of water vapor is present in the air, the values given by equation (25) would be reduced still further so that most of the values given in table 10A would be larger than those given by equation (25). However, from the standpoint of safety, it would be wise to use the more conservative figures given in the above table.

Intertank separation. Again, assuming all the liquid hydrogen in a container can be spilled over a wide area and vaporized quickly to form flammable mixtures with air and that these can be ignited and burned quickly, the maximum diameter of the flame that would be produced is given by equation (14). However, by limiting the spill area with dikes the vaporization rate and the effective flame diameter can be reduced appreciably; the effective flame diameter is reduced to essentially the diameter of the diked area. If we take this to be approximately 0.1 the value given by equation (14), then the diameter of the flame should not exceed the value

$$d \approx \sqrt{|M|} \text{ ft.} \quad (26)$$

This would give a theoretical liquid depth of approximately 1 inch which could be vaporized rather quickly (fig. 5, p. 8). A plot of d is given in figure 38 for M between 10 and 10^5 pounds. In practice, it would be desirable to use an even smaller dike diameter for large tanks (that is, that obtained from equation (24)) so that the effective flame diameter would be less than that given by equation (26). One possible arrangement is to use a concentric dike system. The first dike would enclose a 6-inch pebble bed and would be designed to quickly vaporize small volumes (small leakage rate); the area of this dike should be approximately equal to the area of the storage tank. The second, outer dike should be designed to vaporize large volumes at a slower rate, thus decreasing the rate at which hydrogen would be burned. Under these conditions, the d values of equation (26) should serve as a conservative estimate of the intertank separation. Although the effect of wind has not been considered, the above values of d are quite conservative and should be applicable even in very windy areas. These values were used to compile table 10B.

Personnel who work in the vicinity of liquid hydrogen systems should wear impervious, fire-resistant clothing that can be removed readily if necessary. Adequate head and face protection should not be overlooked. In general, if an accidental spill occurs, the affected area should be evacuated immediately.

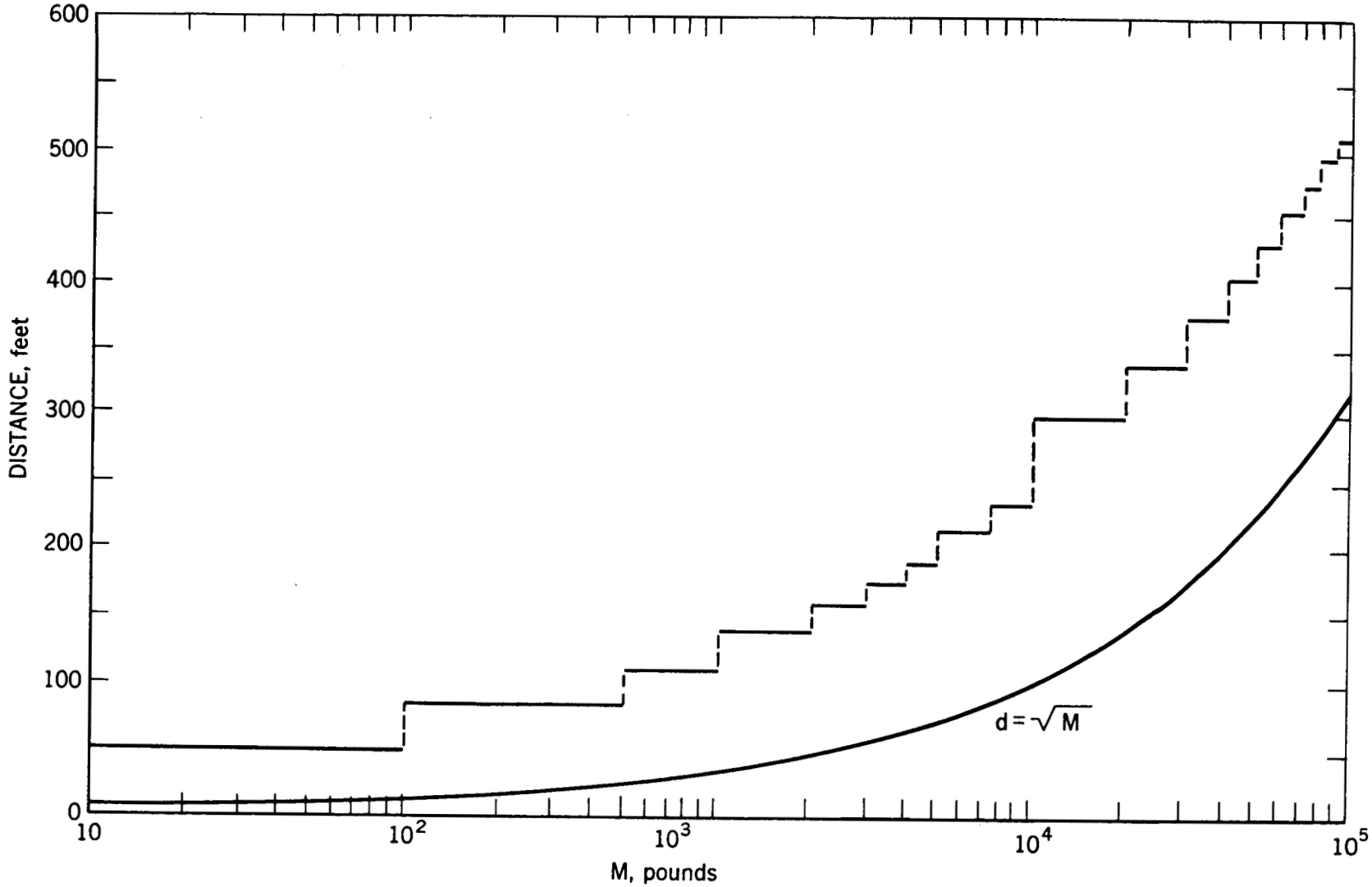

FIGURE 38. - Variation in Above Ground Unbarricaded Intermagazine Separation (Class 950 Materials) and $-\sqrt{M}$ With Mass (M) of Liquid Hydrogen.

APPENDIX I

TABLE 1. - Properties of Hydrogen

Molecular weight..... 2.0162

Density of gas at 32° F.[1/]... 0.08988 g./l. = 0.005611 lb./ft.^{3}

Density of gas at -423° F.[2/]. 1.203 g./l. = 0.07510 lb./ft.^{3}

Boiling point..... -423.0° F. = 36.7° R. = -252.8° C. = 20.4° K.

Density of liquid at -423° F. 70 g./l. = 4.37 lb./ft.^{3} = 0.584 lb./gal.

Specific volume of liquid at -423° F..... 0.0143 l./g. = 0.229 ft.^{3}/lb. = 1.71 gal./lb.

Heat of vaporization..... 213 cal./mole = 7.40 kcal./l. = 190 B.t.u./lb.

Heat of combustion..... 68.37 kcal./mole = 2400 kcal./l.= 61,720 B.t.u./lb.

Heat of conversion..... 339 cal./mole = 11.77 kcal./l. = 303 B.t.u./lb.

1/ Density of air at 32° F.: 1.1573 g./l. = 0.07225 lb./ft.^{3}

2/ Calculated assuming ideal gas behavior.

TABLE 2. - Comparison of measured flame temperatures with values calculated from percentages of heat radiated

Fuel	Measured flame surface temperature, °K.	Percentage radiated	Calculated surface temperature, °K.
Gasoline.....	1/ 1520	42	2/ 1550
Ethylene.....	3/ 1720 1570	36	1780

1/ Rasbash, D. J., Rogowski, Z. E., and Stark, G. W. V., Properties of Fires of Liquids: Fuel, 35, 1956, pp. 94-107.

2/ Gasoline assumed to be n-heptane for purposes of this calculation.

3/ Measured at two points in flame. Details of measurement to be included in Final Report to American Gas Association on Project ZC-20, Chemistry of Very Rich Fuel-Air Flames, by J. M. Singer and J. Grumer. In print.

TABLE 3. - Absorption of flame radiations by 0.116-inch path-length of liquid fuel in cell with CaF_2 windows

Fuel	Percentage absorption
Methanol	100
UDMH	>98
Benzene	60
Hexane	71

TABLE 4. - Influence of cross wind on fuel consumption rates in trays (fuel level about 1/8-inch below rim of tray)

Fuel	Tray dimensions, inches	Wind velocity,[1] feet per second	Burning rate, centimeter per minute	Remarks
Methanol	5-1/2 x 5-1/2	0	0.08	
		5	0.10	
		9	0.10, .14	
		11	0.13, .14	Torn
	4 x 9	9	0.131	Torn
	9 x 4	10	0.133	Torn
Benzene	4 x 9	0	0.19	
		2	0.24	
		4	0.25	
		9	0.27	
		11	0.25	Torn
		11-1/2	0.23	Torn
		>11-1/2	Blowoff	
Hexane	4 x 9	0	(0.15)	Estimated from rate in round tray
		2	0.21	
		4	0.18	
		9	0.21	
	12, diameter[2]	0	[3]/0.35	
		4	[3]/0.30	
		8	[3]/0.29	Torn
	30, diameter[2]	0	[3]/0.49	
		5	[3]/0.56	
		10	[3]/0.61	Torn

1/ Average of wind velocities at front and rear edges of tray.
2/ Measurements made out-of-doors with some interference by wind gusts.
3/ Measured as described in experiments with hydrogen but with only one thermopile.

TABLE 5. - Preliminary measurements of radiative heat transfer in methanol flames

Vessel	Position of probe	Radiant flux, watts per square centimeter
Glass--66-millimeter inside diameter	Center	0.32
Do	Side	0.15
Metal--1-foot diameter	Center	0.32
Do	1 inch from leeward edge	0.29
Do	3-1/2 inch from leeward edge	0.33
Do	2-inch from windward edge	0.27

TABLE 6. - Radiation by gaseous diffusion flames

Fuel	Burner diameter, inches	100 x radiation output, Thermal output (percent)	Fuel	Burner diameter, inches	100 x radiation output, Thermal output (percent)
Carbon monoxide	0.20	17.6	Butane	0.20	21.5
	0.36	17.6		0.36	25.3
	0.73	21.4		0.73	28.6
	1.6	23.4		1.6	28.5
	3.3	23.1		3.3	29.1
	8.0	16.2		8.0	28.0
	16.0	16.5		16.0	29.9
Hydrogen	0.20	9.5	Methane	0.20	10.3
	0.36	9.1		0.36	11.6
	0.73	9.7		0.73	16.0
	1.6	11.1		1.6	16.1
	3.3	15.6		3.3	14.7
	8.0	15.4			
	16.0	16.9			
Ethylene	0.20	27.5	Natural gas (95 percent CH_4)	8.0	19.2
	0.36	27.8		16.0	23.2
	0.73	35.3			
	1.6	38.3			
	3.3	38.4			
	8.0	31.9			
	16.0	35.8			

TABLE 7. - Emissivity of hydrogen diffusion flame on 16-inch burner

Assumed flame temperature, °K.	Average emissivity
2320	0.0046
1900	0.01
1700	0.015
1600	0.02

TABLE 8. - Radiation by liquid-supported diffusion flames

Fuel	Vessel diameter, inches	$\frac{\text{Radiation output}}{\text{Thermal output}} \times 100$, percent
Methanol	1	11.7
	2	14.3
	3	16.2
	6	16.5
	48	12.7
	48	1/ 17.0
Ethanol	3	19.1
	6	19.5
Benzene	2	37.8
	3	35.0
	18	34.5
	30	35.0
	48	36.0
Butane	12	19.9
	18	20.5
	30	26.9
Hydrogen	13	25

1/ Corrected for absorption by atmospheric moisture.

TABLE 9. - Percentage absorption of flame radiations by water vapor (steam at 100° C.) in cells with CaF_2 windows

Burning fuel	Percentage absorption	
	Cell length, 3-1/2-inches[1/]	Cell length, 7-inches[2/]
Hydrogen	33	45
UDMH	18	-
Methanol	13	-
Hexane	1-6	-

1/ Considered comparable to 12-ft. path with water vapor at 15 mm. partial pressure and 25° C.

2/ Considered comparable to 24-ft. path with water vapor at 15 mm. partial pressure and 25° C.

TABLE 10. - Proposed quantity-distance tables for liquid hydrogen

(A) Distance to inhabited buildings			(B) Distance between storage tanks		
Pounds		Distance	Pounds		Distance
Over	Not over	(feet)	Over	Not over	(feet)
0	200	100	0	2,000	50
200	1,000	150	2,000	10,000	100
1,000	5,000	200	10,000	20,000	150
5,000	20,000	250	20,000	40,000	200
20,000	40,000	300	40,000	60,000	250
40,000	100,000	350	60,000	100,000	300

APPENDIX II

Cryostat and Associated Equipment

The layout of the Collins Cryostat and the related equipment is shown schematically in figure 39. The cryostat, two four-stage compressors, the gasholder and helium cylinders were set up in one area and the hydrogen-supply and liquid-hydrogen dewars in a separate adjacent area that is covered by a hood and vented by a vertical 20-inch stack leading through the hood. A fan shown at the left in the figure is located near the ceiling to prevent the accumulation of hydrogen that escapes from the hooded area or from the cryostat.

A commercial gas analyzer was adapted for use in detecting leaks in the above system. A hydrogen buildup to 0.5 percent in any of the five areas above the working area or near the exhaust fan causes the equipment to sound an audible alarm. The unit was found to work satisfactorily; hydrogen leaks were detected on several occasions with this arrangement.

In practice, approximately one hour is required to initiate liquefaction after startup of the cryostat. By precooling the hydrogen stream with liquid nitrogen just before it enters the cryostat, a liquefaction rate of 6 to 6.5 liters of hydrogen per hour is achieved.

The liquid hydrogen is transferred from the cryostat through an evacuated transfer line; helium is used to pressurize the space above the liquid and effect the transfer. The amount of liquid produced during a run is calculated from the volume of gas fed into the system; this figure is checked by the use of a resonance-type liquid-level indicator.

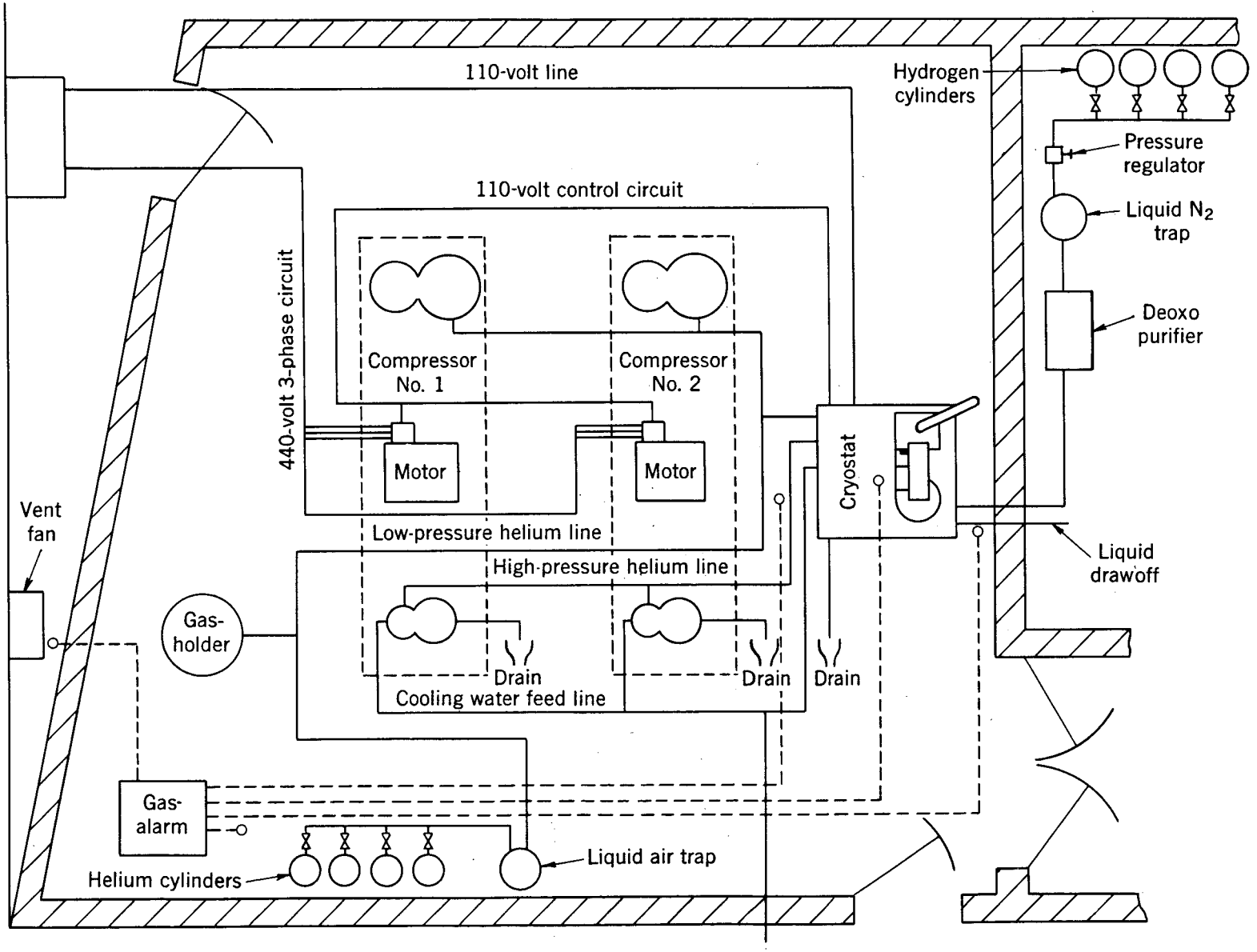

FIGURE 39. - Schematic Layout of Collins Cryostat and Related Equipment.

APPENDIX III

Measurement of Liquid Burning Rates

The burning rates quoted for liquid hydrogen all depend on an assumption that the instantaneous level of radiation from the flame is proportional to the burning rate at the same point in time. Then if one knows the total duration of the burning and the total depth of liquid consumed, and has a record of radiation versus time, it is a simple problem of proportionality to construct a curve of burning rate versus time. The radiation records were taken with two or three Eppley thermopiles.

This method was tested with the conventional fuels against several direct methods of measurement: (1) With methanol flames one can observe the liquid visually. A pointer can be observed to touch (dimple) the surface and fuel is added to the burner at such a rate as to maintain this contact. The burning rate is then determined from the measured addition rate of fuel. (2) With methanol and benzene the liquid level can be allowed to recede past an array of vertically-spaced thermocouples. As each thermocouple breaks the surface there is an immediate rise in temperature of several hundreds of degrees. The resolution in time of this emergence is within 2 seconds. With hydrogen and butane flames no sharp break in temperature is observed as the thermocouples emerge from the liquid phase into the vapor phase. (3) With water-insoluble fuels, that is, benzene, hexane, and butane, measured volumes of fuel can be poured onto water and allowed to burn to completion. Several depths of liquid, for example, 1, 2 and 4 inches, are burned to comprise each burning rate determination.

None of these direct methods of measuring the surface level is applicable to burning of liquid hydrogen. However, the assumption that radiation level is proportional to burning rate was found satisfactory with each of the five common fuels, with burning rate established independently by one or more of the direct methods.

APPENDIX IV

Radiation Measurements

An instrument devised here for measuring radiation to the liquid surface is shown in figure 40. The entire capsule containing the differential (shielded-unshielded) thermocouple is immersed in the burning fuel and e.m.f. readings are taken as the liquid level approaches the tip of the thin-blown pyrex shield. The readings increase to a plateau value which is maintained until the liquid level approaches that of the silver shield whereupon readings break sharply upward. Presumably, this "break" corresponds to heating of the pyrex which in turn acts as a radiation source. The plateau value of e.m.f. is used as an indication of radiation received. The chief obstacle to further refinement and use of the device is the problem of calibration--only a source of the same wavelength distribution as that of the flame can be used. However, it is felt that the measurements shown in table 5 are of the right order of magnitude and the method should be applicable to the study of other fuel-flame systems.

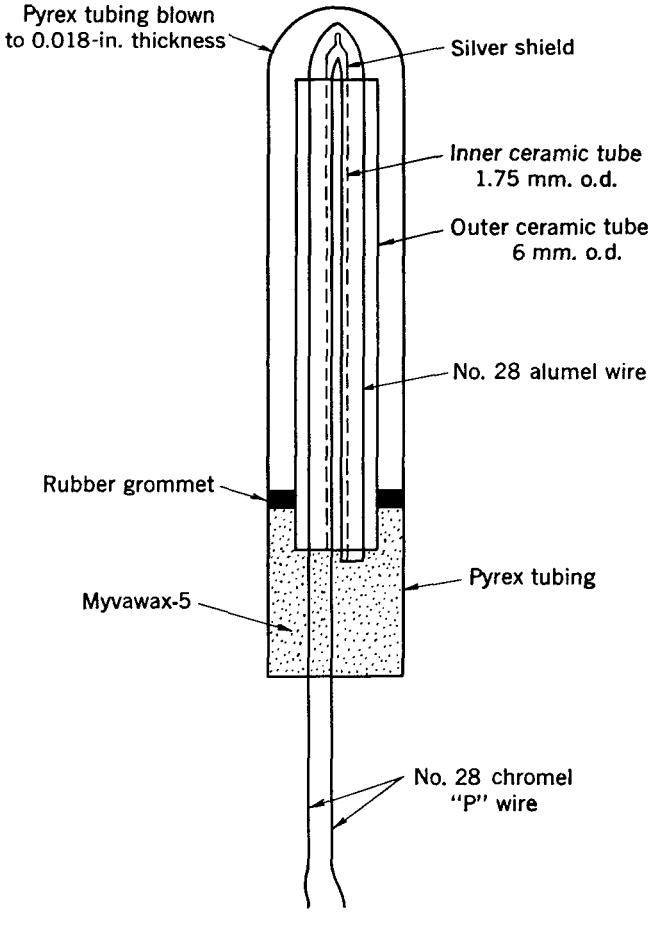

FIGURE 40. - Compensated Thermocouple for Radiation Measurements.

INT.-BU.OF MINES,PGH.,PA. 2053